DIGITAL ACCESS TO
SCHOLARSHIP AT HARVARD
DASH.HARVARD.EDU

HARVARD LIBRARY
Office for Scholarly Communication

The mTORC1/4E-BP pathway coordinates hemoglobin production with L-leucine availability

The Harvard community has made this article openly available. **Please share** how this access benefits you. Your story matters

Citation	Chung, J., D. E. Bauer, A. Ghamari, C. P. Nizzi, K. M. Deck, P. D. Kingsley, Y. Y. Yien, et al. 2015. "The mTORC1/4E-BP Pathway Coordinates Hemoglobin Production with L-Leucine Availability." Science Signaling 8 (372) (April 14, 2015): ra34–ra34. doi:10.1126/scisignal.aaa5903.
Published Version	doi:10.1126/scisignal.aaa5903
Citable link	http://nrs.harvard.edu/urn-3:HUL.InstRepos:33758681
Terms of Use	This article was downloaded from Harvard University's DASH repository, and is made available under the terms and conditions applicable to Open Access Policy Articles, as set forth at http://nrs.harvard.edu/urn-3:HUL.InstRepos:dash.current.terms-of-use#OAP

The mTORC1/4E-BP pathway coordinates hemoglobin production with L-leucine availability

Jacky Chung[1], **Daniel E. Bauer**[2,3], **Alireza Ghamari**[2,3], **Christopher P. Nizzi**[4], **Kathryn M. Deck**[4], **Paul D. Kingsley**[5], **Yvette Y. Yien**[1], **Nicholas C. Huston**[1], **Caiyong Chen**[1,†], **Iman J. Schultz**[1,†], **Arthur J. Dalton**[1], **Johannes G. Wittig**[1,†], **James Palis**[5], **Stuart H. Orkin**[2,3], **Harvey F. Lodish**[6], **Richard S. Eisenstein**[4], **Alan B. Cantor**[2,3], and **Barry H. Paw**[1,2,3,*]

[1]Division of Hematology, Brigham & Women's Hospital, Harvard Medical School, Boston, MA 02115, USA

[2]Division of Hematology-Oncology, Boston Children's Hospital, Harvard Medical School, Boston, MA 02115, USA

[3]Department of Pediatric Oncology, Dana-Farber Cancer Institute, Harvard Medical School, Boston, MA 02115, USA

[4]Department of Nutritional Sciences, University of Wisconsin-Madison, Madison, WI 53706, USA

[5]Department of Pediatrics, University of Rochester Medical Center, Center for Pediatric Biomedical Research, Rochester, NY 14642, USA

[6]Whitehead Institute for Biomedical Research, Massachusetts Institute of Technology, Cambridge, MA 02142, USA

Abstract

In multicellular organisms, the mechanisms by which diverse cell types acquire distinct amino acids and how cellular function adapts to their availability are fundamental questions in biology. Here, we found that increased neutral essential amino acid (NEAA) uptake was a critical component of erythropoiesis. As red blood cells matured, expression of the amino acid transporter gene *Lat3* increased, which increased NEAA import. Inadequate NEAA uptake by pharmacologic inhibition or RNAi-mediated knockdown of LAT3 triggered a specific reduction in hemoglobin production in zebrafish embryos and murine erythroid cells through the mTORC1 (mechanistic target of rapamycin complex 1)/4E-BP (eukaryotic translation initiation factor 4E-binding protein) pathway. CRISPR-mediated deletion of members of the 4E-BP family in murine erythroid cells

*To whom correspondence should be addressed: Barry H. Paw, Division of Hematology, Brigham & Women's Hospital, 1 Blackfan Circle, Karp Bldg, 05.211, Boston MA 02115, Tele: (617) 355-9008; bpaw@rics.bwh.harvard.edu.
†Present address: C.C., Zhejiang University, Hangzhou 310058, China; I.J.S., InteRNA Technologies, 3584 CH Utrecht, The Netherlands; J.G.W., Technische Universität Dresden, BIOTEChnologisches Zentrum, Dresden 01307, Germany.

rendered them resistant to mTORC1 and LAT3 inhibition and restored hemoglobin production. These results identify a developmental role for LAT3 in red blood cells and demonstrate that mTORC1 serves as a homeostatic sensor that couples hemoglobin production at the translational level to sufficient uptake of NEAAs, particularly L-leucine.

Introduction

Amino acids are the fundamental building blocks of all proteins. Clinically, targeting amino acid metabolism is gaining increasing prominence as a treatment modality for several human diseases (1–4), highlighting the need for a more thorough basic understanding of amino acid metabolism in normal physiology. For most eukaryotes that lack the ability to produce essential amino acids (EAA) *de novo*, transport mechanisms are required for uptake of EAAs from the extracellular *milieu* (5). There are several classes of EAA transporters, one of which is the System L ('leucine preferring') family that consists of four members – LAT1 (SLC7A5), LAT2 (SLC7A6), LAT3 (SLC43A1), and LAT4 (SLC43A2) (6–8). LAT1 and LAT2 have broader substrate specificity and require the CD98 (SLC3A2) co-transporter for function whereas LAT3 and LAT4 are monomeric facilitative uniporters with greater affinity for the transport of branched, neutral essential amino acids (NEAAs) particularly L-leucine (6, 7, 9, 10). To date, the vast majority of work has focused on unravelling LAT1 function (7, 11–14), and little is known regarding the roles of other LAT-family proteins in normal development (6).

Eukaryotic cells adapt to insufficient EAA uptake by altering their cellular metabolism (5). One such mechanism, which was first identified in yeast and later in mammals, involves the activation of the kinase GCN2 (general control nonderepressible 2) by uncharged tRNAs under severe amino acid deprivation (15–17). Active GCN2 inhibits eIF2α (eukaryotic initiation factor 2α) by phosphorylating Ser^{51}, thereby decreasing global translation initiation (18–20). Paradoxically, phosphorylated eIF2α also triggers the translation of a subset of mRNAs including *Atf4* (15, 16, 21, 22), which encodes a transcription factor that induces the expression of genes involved in amino acid metabolism to increase amino acid availability (19, 23). The serine/threonine kinase mTORC1 constitutes a second pathway that is responsive to amino acid stress, particularly L-leucine deficiency (24–26). Under nutrient rich conditions, mTORC1 is active and phosphorylates various downstream proteins that mediate anabolic metabolism including activation of protein translation (24–29). When nutrient pools, particularly L-leucine, become depleted, mTORC1 activity diminishes, triggering cellular catabolism (3, 24–26). Although mTORC1 activity can be modulated by L-leucine-loaded leucyl-tRNA synthetase (30, 31), it is also sensitive to changes in the intracellular L-leucine pool (24, 25). This indicates that a hierarchy exists in amino acid stress responses such that mTORC1 responds to variations in amino acid pools, particularly L-leucine, while GCN2 is only engaged under general severe starvation conditions.

Efforts to decipher mTORC1 translation control have relied upon pharmacologic and genetic loss-of-function approaches (27, 28, 32). However, such pronounced deficiencies in mTORC1 activity are unlikely to be encountered physiologically and does not accurately reflect feedback regulation of maintaining nutrient homeostasis. This is an essential

consideration in understanding the physiologic role of mTORC1 signaling that may have a substantial impact on biological output (33). For example, phosphorylation of eIF2α inhibits the translation of most proteins (18–20), but particularly that of *globin* transcripts in erythroid cells (34). This is largely due to feedback regulation of heme availability that signals to intricately balance α/β-globin protein translation to heme biosynthesis (34) and the vast number of globin proteins that comprise 97% of the erythroid proteome (35).

In humans, mutations in the translation machinery are associated with approximately 50% of Diamond-Blackfan Anemias (DBAs) while the remaining anemias have unknown causes (36–38). Modulation of the mTORC1 pathway has been reported to alleviate DBA symptoms in model organisms (39). Together, these results not only underscore the importance of translational regulation in erythropoiesis but also the need to better understand the dynamics of nutrient homeostasis. This knowledge can substantially impact human health by uncovering potentially new causes of disease as well as improved treatment options. Here, we show that red blood cell development requires increased NEAA uptake and mTORC1 coordinates hemoglobin production with the availability of NEAAs, particularly that of L-leucine.

Results

Erythropoiesis involves increased NEAA uptake through LAT3

As erythrocytes mature, their transcriptional profile undergo changes that reflect an altered metabolic state, including the induction of iron and heme metabolism genes, as well as those involved in amino acid recycling (40–43). The maintenance of amino acid homeostasis plays a critical role in erythropoiesis (42), highlighting how red blood cell development serves as an excellent framework for understanding the metabolic regulation of amino acid signalling during normal physiology. Using RNAseq (44, 45), we found that the expression of mRNAs encoding System L amino acid transporters, *Lat1* (also known as *Slc7a5*) and *Lat3* (also known as *Slc43a1*), were substantially increased in maturing red blood cells in a manner similar to mRNAs for other erythroid solute transporters such as *Glut1* (also known as *Slc2a1*), *Ae1* (also known as *Slc4a1*), and *Mfrn1* (also known as *Slc25a37*); iron- and heme-metabolism genes such as *Tfrc*, *Snx3*, and *Fech*; and other erythroid-associated genes such as *Hba-a1* (which encodes α-globin) and *Hbb-b1* (which encodes β-globin) (Figure 1A) (45). The transcript abundance of two closely related paralogs (6), *Lat2* (also known as *Slc7a6*) and *Lat4* (also known as *Slc43a2*), or the *Tuba1a* gene (which encodes the cytoskeletal protein β-tubulin) were relatively unchanged throughout erythroid maturation (Figure 1A). We also did not detect expression of the mRNA encoding CD98 co-transporter requisite for LAT1-dependent transport, indicating that although it was induced, LAT1 was likely not functional. Thus, we focused our subsequent analysis on *Lat3*.

In situ hybridization performed on the developing murine embryo revealed broad expression of *Lat3* at E8.5 with enrichment in erythropoietic blood islands of the yolk sac as well as the neural epithelium (Figure S1A) and highly expression in the fetal liver, the site of definitive erythropoiesis, at E14.5 (Figure 1B). The *Lat3* expression pattern mirrors that of heme metabolism genes (46, 47). *LAT3* transcript abundance was also increased in human CD34$^+$ cells induced to differentiate along the erythroid lineage (Figure S1B). We also examined

changes in *Lat3* expression in differentiating Friend murine erythroleukemia (MEL) cells, which are committed erythroid cells that are used to study red blood cell maturation (48). Consistent with our observations in the murine embryo, the abundance of the mRNA and protein increased in terminally differentiating MEL cells (Figures 1C and D). Further analysis of ChIP-sequencing databases for the erythroid master transcription factors GATA-1 and KLF1 revealed the presence of GATA-1 (49) and KLF1 (50, 51) binding sites within intron 1 and the promoter of the murine *Lat3* gene, respectively, suggesting that *Lat3* is directly induced by erythroid master transcription factors during erythropoiesis.

Given the increase in *Lat3* expression, we tested whether maturing red blood cells exhibited increased uptake of NEAAs. LAT3 most efficiently transports L-leucine compared to other substrates such as L-phenylalanine, L-isoleucine, L-valine, and L-methionine (9). Thus, we performed uptake assays using L-leucine as a representative amino acid. Differentiating MEL cells took up more [^{3}H]-L-leucine than undifferentiated cells, an effect that was restored to basal amounts with 2-aminobicyclo-(2,2,1)-heptane-2-carboxylic acid (BCH) (Figure 1E), a System L-specific plasma membrane inhibitor (6). BCH also partially blocked L-leucine uptake in differentiating primary murine fetal liver cells (Figure S1C). Stable knockdown of *Lat3* expression with shRNAs in maturing MEL cells similarly diminished but did not fully abrogate [^{3}H]-L-leucine import (Figures 1F to H). In contrast, competition assays showed that [^{3}H]-L-leucine uptake was markedly decreased by the addition of excess, non-radioactive L-leucine, partially decreased by the addition of other NEAAs, and not affected by D-leucine, L-glutamic acid, or L-glutamine (Figure 1I), indicating that maturing erythroid cells have higher NEAA import mediated by increased expression of *Lat3* but that basal transport relies on other mechanisms or transporters (6). Gas chromatography-mass spectrometry (GC-MS) analysis also demonstrated that intracellular concentrations of L-leucine as well as L-phenylalanine, L-valine, and L-isoleucine – all purported substrates of LAT3 (9) – were decreased in *Lat3* shRNA-expressing erythroid cells that were differentiated (Figure 1J), but not those that were undifferentiated (Figure S1D). However, our analysis of differentiating cells did not find any significant difference in L-methionine concentrations (Figure 1J), consistent with previous work showing that L-methionine is a relatively poor substrate although it can efficiently outcompete LAT3-mediated transport of other NEAAs (9). In addition, undifferentiated, *Lat3* shRNA-expressing cells showed no difference in [^{3}H]-L-leucine import from controls (Figure S1E). Together, our data indicate that increased LAT3-mediated NEAA import during red blood cell maturation is a component of developmental erythropoiesis.

Hemoglobin production is coupled to NEAA sufficiency

The increase in LAT3-mediated NEAA uptake in maturing erythroid cells prompted us to examine how cells adapt to amino acid stresses *in vivo* with the zebrafish (*Danio rerio*) model that has been widely used to study hematopoiesis. Although mammals have only one *Lat3* gene, a GenBank BLAST query revealed that zebrafish have two *Lat3* paralogs – *lat3a* (*slc43a1a*) and *lat3b* (*slc43a1b*) – which are likely to have arisen because of genomic duplication during teleost evolution (Figure S2A) (52). In some cases, gene duplication in teleosts has facilitated the study of cell-type specific effects by circumventing early embryonic lethality from global loss-of-function effects (53). *In situ* hybridization

performed on 24 hours post-fertilization (hpf) zebrafish embryos indicated that zygotic *lat3a* transcripts, but not *lat3b*, can be readily detected at the 20 somite stage in the intermediate cell mass (ICM) which is equivalent to the mammalian primitive erythropoietic blood islands and is characterized by *gata-1* expression (Figures 2A and S2B). *lat3a* ICM staining was further confirmed by performing *in situ* hybridization on 24 hpf *chordino* (*dino*) (54) or *spadetail* (*spt*) (55) mutants which either have an expanded or absent blood progenitor population, respectively. The *lat3a* staining pattern paralleled that of *gata-1* with increased ICM staining in the *dino* mutants and no ICM staining in *spt* mutants (Figure 2B), indicating that *lat3a* is the functional ortholog in zebrafish erythropoiesis while *lat3b* is required for zebrafish nephrogenesis as previously reported (56).

Because naïve *Lat1*$^{-/-}$ T-cells with inadequate NEAA import fail to differentiate (7), we asked whether limiting NEAA uptake in erythroid cells by inhibiting LAT3 function affected lineage commitment and specification. Using a transgenic zebrafish line that expresses enhanced green fluorescent protein (eGFP) driven by the *globin* promoter (Tg(*globin-LCR*:eGFP)), *lat3a* morphants had a comparable proportion of erythroid cells as control zebrafish embryos at 48 hpf (Figures 2C and D). However, at 72 hpf, we noticed a decrease in eGFP-positive erythroid cells in these morphant embryos (Figure 2D). In contrast, a second transgenic zebrafish line that expresses eGFP driven by the *gata-1* promoter (Tg(*gata-1*:eGFP)) showed a slight increase (that was not statistically significant) in the proportion of Tg(*gata-1*:eGFP)-positive erythroid cells in *lat3a* morphants (Figure 2E), which may represent compensatory erythropoiesis that has previously been documented in models of defective red blood cell development (57, 58). In support of this notion, the proliferation of maturing MEL cells expressing either *Lat3* shRNA was higher than in control cells (Figure S2C). Together, these data suggest that LAT3 inhibition does not adversely affect erythroid specification and that the reduction in erythroid numbers in Tg(*globin-LCR*:eGFP) transgenic morphants represents a specific decrease in globin protein abundance. We further tested this idea by examining additional erythroid markers by *in situ* hybridization. Control and *lat3a* morphants expressed comparable amounts of the early erythroid markers *gata-1* (59) and *ae1* (60) at 24 and 48 hpf (Figures S2D and E), respectively. Analysis of thrombocytic, myeloid, and lymphoid populations in *lat3a* morphants did not reveal a substantial effect on other hematopoietic lineages (Figures S2F to H), suggesting that NEAA insufficiency did not affect hematopoietic lineage commitment or specification. We used flow cytometry analysis to further examine whether NEAA availability influences differentiation within the erythroid lineage. Primary murine fetal liver cells expressing *Lat3* shRNAs showed no significant differences in the proportion of c-KIT^{High};TER119^{Low} progenitors or more committed c-KIT^{Moderate};TER119^{High} and c-KIT^{Low};TER119^{High} erythroid populations (Figures S2I to K). In addition, both control and *Lat3* shRNA-expressing cells had similar increases in GATA-1 protein abundance (Figure S2L), though this result differs slightly from that of a previous study showing a lack of change in GATA-1 abundance throughout MEL cell maturation (61), a difference that likely reflects genetic drift of our MEL cell subclone.

While NEAA insufficiency did not affect red blood cell commitment and specification, the decrease in eGFP-positive cells in Tg(*globin-LCR*:eGFP) morphants (Figure 2D) suggested

a reduction in globin protein production. We directly tested this idea by performing *o*-dianisidine staining, which a substantial reduction in red blood cell hemoglobinization in *lat3a* morphants (Figure 2F). This effect was specific for *lat3a* because knockdown of the only zebrafish *lat1* homolog did not affect hemoglobinization (Figures S2M and N) although *lat1* expression was increased in murine fetal liver cells (Figure 1A) and in the ICM of 24 hpf zebrafish embryos (Figure S2O). This finding agrees with LAT1's functional requirement for the CD98 co-transporter, which is not present in erythroid cells (6). Pharmacologic inhibition or RNAi-mediated knockdown of LAT3 in MEL and primary murine fetal liver cells similarly reduced the proportion of *o*-dianisidine-positive cells (Figures 1F, G, and 2G to J), indicating that hemoglobin production in red cells requires adequate LAT3-dependent NEAA uptake. These data are also consistent with the expression profile of *Lat3* (Figure 1A) in which maximal *Lat3* expression occurs at latter stages of erythroid maturation when hemoglobinization becomes most prominent (62).

Nascent globin protein translation depends on NEAA availability

We began to explore the molecular mechanisms and specificity underlying the deficit in hemoglobin production in response to limited NEAA uptake by first examining the abundance of erythroid-specific proteins (Ankyrin1 and EPB42) and mitochondrial heme biosynthetic enzymes (ALAS2, PPOX, and FECH) that are critical for erythroid maturation (Figure 3A) (63, 64). The protein abundance of all markers was similar in control and *Lat3* shRNA-expressing maturing erythroid cells (Figure 3A), as was that of several housekeeping proteins (TUBA1A, GAPDH, HSPD1, COX-IV) (Figure 3A). Mitochondrial physiology was also unaffected in maturing red blood cells with LAT3 knockdown since we did not detect deficiencies in mitochondrial biogenesis and glycolytic and TCA cycle intermediates (Figures S3A to C). These findings suggest that overall cellular function was largely unaffected by *Lat3* knockdown. However, we noticed a substantial reduction in the abundance of α-globin protein (Figure 3B) despite robust mRNA expression (Figures 3C and S3D). Unfortunately, we were unable to analyze β-globin protein abundance due to the lack of an immunoblot-applicable antibody. A similar decrease in β-globin protein abundance is likely since an imbalance in the ratio of α and β globin chains is cytotoxic and would lead to a substantial decrease in cell viability (65), which was not observed in either maturing primary murine fetal liver or MEL cells with LAT3 knockdown (Figures S3E and F). Moreover, although *Lat3*-shRNA expressing cells had lower TFRC protein abundance, iron uptake, and heme-bound iron, exogenous non-transferrin bound iron supplementation did not restore hemoglobinization in these cells, but could do so in a *SNX3*-silenced MEL clone (Figures S3G to J), which has a defect in the efficient acquisition of transferrin-bound iron (47). These findings exclude primary iron deficiency as the cause for the decreased hemoglobin production and suggests that NEAA insufficiency leads to a selective decrease in α/β-globin protein translation.

To test this idea, we performed non-radioactive metabolic labeling experiments with the L-methionine analog L-azidohomoalanine (L-AHA) (37). Metabolic labeling provides the most robust and accurate measurement of changes in protein translation rate (37, 66). We found that *Lat3* knockdown substantially compromised nascent α/β-globin protein synthesis without affecting general translation, as evidenced by comparable amounts of higher

molecular weight bands and similar steady-state amounts of several housekeeping proteins (Figure 3D). In support of this notion, complementary polysome profiling revealed that *α/β-globin* mRNAs, but not those of other genes (Figure 3E and F) were shifted to lighter polysome fractions associated with decreased translation initiation in *Lat3*-shRNA expressing maturing erythroid cells (20, 66). Given the sheer abundance of *α/β-globin* transcripts in red blood cells (35), even a selective reduction in α/β-globin translation results in a global decrease in polysome size (Figure 3E), an effect that has previously been reported (67). Together, our results are consistent with a selective decrease in the translation α/β-globin proteins caused by diminished translation initiation that is associated with lighter polysomes and not elongation or termination which would similarly result in slower translation but paradoxically with higher density polysomes (66, 68–72). To further establish the causal relationship between α/β-globin protein translation and subsequent change in steady-state amounts, we performed metabolic labeling experiments on already-differentiated MEL cells. Short-term treatment with BCH to acutely inhibit LAT3 function significantly reduced nascent α/β-globin protein synthesis before a noticeable effect on steady-state α-globin protein abundance (Figure 3G). Thus, a specific deficit in globin protein translation occurs *a priori* and causes diminished red blood cell hemoglobinization under conditions of NEAA insufficiency.

mTORC1 senses sufficient uptake of NEAAs, particularly L-leucine, in maturing erythroid cells

Although LAT3 can transport L-leucine, L-phenylalanine, L-valine, and L-isoleucine, we wondered if a particular amino acid was more important for red cell hemoglobinization and tested this by administering esterified derivatives of these amino acids individually to BCH-treated MEL cells. Esterified amino acids are lipid permeable and, once inside the cell, are converted to usable proteinogenic amino acids by endogenous esterases (73). *o*-dianisidine staining revealed that esterified L-leucine had the most pronounced effect at restoring hemoglobin production (Figure 4A). In addition, metabolic labeling experiments showed that esterified L-leucine most effectively increased the rate of α/β-globin protein translation in BCH-treated MEL cells (Figures 4B and C). This suggests that although LAT3 transports multiple NEAAs, hemoglobin production in maturing erythroid cells is particularly sensitive to L-leucine availability.

The responsiveness to L-leucine content and the preferential reduction in α/β-globin protein translation suggests that this is a coordinated adaptive mechanism that enables maturing erythroid cells to cope with amino acid insufficiency. The mammalian target of rapamycin complex 1 (mTORC1) is a kinase that is sensitive to amino acid availability, particularly that of L-leucine (24–26). Thus, we next asked whether mTORC1 coordinates hemoglobin production with NEAA availability in maturing erythroid cells by examining whether mTORC1 activity was affected by LAT3 inhibition. Phosphorylation of Thr[37/46] in 4E-BP1 and Thr[389] in S6K1 – two well-characterized mTORC1 targets – as well as phosphorylation of Ser[240/244] in S6 were decreased in differentiating *Lat3*-knockdown MEL cells (Figure 4D). The phosphorylation of S6K1 was not altered in undifferentiated cells (Figure S4A). These findings are consistent with the dispensable role for LAT3 in undifferentiated red blood cells (Figures S1D and E). Additionally, MEL cells expressing *Lat3* shRNAs also had

increased autophagy characterized by higher LC3-II amounts (Figure 4D), another marker of reduced mTORC1 function. Similarly, *lat3a* zebrafish morphants embryos at both 48 and 72 hpf showed reduced phosphorylation of Thr$^{37/46}$ in 4E-BP1 and of Thr^{389} in S6K1 (Figure 4E). mTORC1 activity was reduced in both undifferentiated and differentiating MEL cells starved of L-leucine, indicating that mTORC1 signaling was intact regardless of erythroid maturation (Figure S4B). In contrast, phosphorylation of Ser^{51} in eIF2α did not change in MEL cells with *Lat3* knockdown (Figure S4C) or in *lat3a* zebrafish morphants (Figure S4D). These results were consistent with the partial reduction in NEAA uptake induced by LAT3 inhibition which did not enable uncharged tRNAs to stimulate the kinase activity of GCN2, which required complete amino acid starvation (Figure S4E) (28) or complete L-leucine starvation which may also reduce hemoglobin production (Figure S4F and G).

To further examine whether mTORC1 activity regulated hemoglobin production, we treated MEL cells with the pharmacological mTOR inhibitors rapamycin and torin 1. MEL cell maturation occurs over four days and hemoglobinization was reduced by continuous, chronic treatment of MEL cells with torin 1, but not with rapamycin (Figures 4F to I). Only an acute, twenty-four hour rapamycin treatment inhibited hemoglobinization (Figures 4H and I). The effect of rapamycin on hemoglobinization correlated with reduced phosphorylation of 4E-BP1, but not of S6K1 (Figures 4H and I), which agrees with work showing that S6K1 phosphorylation is more sensitive to rapamycin-mediated mTORC1 inhibition (28, 74). We also confirmed the effects of mTORC1 inhibition *in vivo*. Treatment with either rapamycin or torin 1 reduced hemoglobinization in zebrafish embryos, with torin 1 having a more pronounced effect (Figures 4J and K). Finally, although esterified L-leucine increased α/β-globin protein translation in MEL cells treated short-term with BCH (Figures 4B and C), it had no effect on torin 1 treated MEL cells (Figure 4L), suggesting that mTORC1 activity is downstream of LAT3 and required for coordinated α/β-globin protein translation in response to L-leucine availability.

α/β-globin transcripts are direct mTORC1 translational targets

mTORC1 is a critical regulator of protein translation and its effects are believed to involve both direct and indirect mechanisms (27, 28). Biochemically, direct mechanisms have been defined as translational changes that occur immediately (within two hours) following mTORC1 inhibition while indirect mechanisms first involve mTORC1-dependent changes in the abundance of ribosomal subunits and would be engaged after the immediate response (27, 28). Transcripts that are directly regulated by mTORC1 also typically, but not always, possess 5′ terminal oligopyrimidine (TOP) or TOP-like mRNA motifs (such as a pyrimidine rich translational element (PRTE)) (27, 28, 66). Given our results that α/β-globin protein translation was dependent on mTORC1 activity, we asked whether α/β-globin transcripts are direct mTORC1 targets by evaluating these two criteria.

First, by mapping the transcription start sites of human and murine *globin* mRNAs using data from RefSeq, ENSEMBL, and UCSC databases, we found that five out of the six *globin* transcripts fit the definitions of a TOP-like motif or PRTE (27, 28) (Figure 5A). Unfortunately, we were unable to confirm our results using the database of transcription start sites (dbTSS) (28) that contain data from experimentally validated transcription start

sites because α/β-globin mRNAs have not yet been annotated in the dbTSS. Nonetheless, all currently available data indicate that α/β-globin transcripts do possess 5′ elements typically associated with direct mTORC1 translational regulation (66).

Examining the sensitivity of α/β-globin protein translation to acute mTORC1 inhibition is the most crucial test of whether they represent direct targets. In fact, the enrichment of TOP and TOP-like variants has been derived using this definition (27, 28, 66). Empirical evaluation of acute responsiveness is required given the potential ambiguity of α/β-globin transcription start sites in the absence of reliable data from dbTSS. Metabolic labeling experiments performed on differentiated MEL cells showed that α/β-globin protein translation was acutely responsive to short-term inhibition of mTORC1 activity by torin 1 (28) before a concomitant change in α-globin protein abundance (Figure 5B). Polysome profiling experiments also confirmed a shift of *α/β-globin* mRNAs to lighter polysome and monosome fractions (Figures 5C and D). Compared to *Lat3* shRNA knockdown (Figures 3E and F), the effects of torin 1 treatment are much more pronounced and widespread (such as depletion of *Gata-1* from polysomes with torin 1 treatment but not with *Lat3* shRNA knockdown), which is consistent with previous data showing that potent and acute mTORC1 inhibition by torin 1 affects the translation initiation of many proteins (28). As previously reported (28), *Ybx1* was shifted to lighter polysome fractions while *Actb* was more refractory to the effects of torin 1 (Figure 5D). Together, our data establish α/β-globin mRNAs as direct, physiologic translational targets of mTORC1.

Control of hemoglobin production is mediated by 4E-BPs

The molecular mechanisms underlying mTORC1 translational regulation have been of considerable interest (27, 28, 75). Accumulating evidence indicates that 4E-BPs, not S6Ks, are the major regulators downstream of mTORC1 that mediate its direct effects (28). Unphosphorylated 4E-BPs bind to eIF4E, blocking the formation of the eIF4F complex to inhibit translation initiation. To date, three 4E-BP proteins have been identified but only two have been studied (4E-BP1 and 4E-BP2) with regards to translation initiation (28, 76). We hypothesized that 4E-BPs were critical regulators of red blood cell hemoglobinization for three reasons: (i) *α/β-globin* transcripts are direct mTORC1 translational targets (Figure 5); (ii) LAT3 inhibition triggers a depletion of α/β-globins from heavier polysome fractions, an effect that reflects diminished translation initiation (Figures 3E to G); and (iii) the effect of pharmacologic mTORC1 inhibition on hemoglobinization correlated with changes in the phosphorylation of 4E-BP1 but not that of S6K1 (Figures 4H and I).

We began testing our hypothesis with the 4E-BP mimetic 4EGI-1 and the S6K inhibitor DG2. Hemoglobin production in MEL cells and zebrafish embryos was reduced by 4EGI-1, but not in MEL cells by DG2 (Figure 6A and B), although phosphorylation of S6 was markedly reduced (Figures S5A), suggesting that control of hemoglobin production largely relies on 4E-BPs, not S6Ks. We further confirmed this result by deleting *4e-bp1* (*Eif4ebp1*) and *4e-bp2* (*Eif4ebp2*) using CRISPR/Cas9 genome editing in MEL cells (Figures S5B to D). Compound, double-knockout (DKO) MEL cells retained greater hemoglobinization (Figures 6C and D) and α/β-globin protein translation (Figures 6E to H) compared to wild-type cells when treated with BCH or torin 1. Notably, loss of 4E-BP proteins had a greater

effect on attenuating the inhibition of hemoglobinization by torin-1 than by BCH (Figures 6C and D). This result is likely because BCH inhibits NEAA uptake, resulting in inadequate NEAA substrate availability, an effect that would not be caused by torin 1 inhibition. Furthermore, administration of esterified L-leucine did not affect the translation rate of α/β-globin proteins in DKO erythroid cells treated with BCH or torin 1 (Figures 6I and J). Chloroquine-treatment to inhibit autophagy (77) also failed to restore hemoglobin production in BCH-treated MEL cells (Figure S5E) as well as the translation and abundance of globin proteins in wild-type and DKO cells (Figure S5F), suggesting that the reduction in globin protein abundance does not result from autophagic hemoglobin degradation. Taken together, our data suggests that integrated NEAA uptake is an integral aspect of erythropoiesis. mTORC1 serves as a sensor for NEAA sufficiency, particularly L-leucine, and coordinately regulates hemoglobin output at the translational level through the 4E-BPs and is distinct from the previously identified HRI signaling pathway (Figure 7). We propose that this likely constitutes an adaptive mechanism in red blood cells because globin proteins have an unusually high L-leucine content compared to many other erythroid-enriched and housekeeper proteins (Figure S5G and Table S1).

Discussion

Why would erythroid cells require such a regulatory mechanism? The unusually high L-leucine content of the globin proteins together with their overall abundance (35) suggests that red blood cells require strategies to coordinate hemoglobin production with the availability of NEAAs, particularly L-leucine. mTORC1 exerts its metabolic effects through several effector pathways (24, 26). In non-erythroid tissues, mTORC1 inhibition reduces TFRC-mediated iron uptake (78). Although this effect may occur in maturing red blood cells (Figures S3G to I), iron supplementation does not appreciably increase hemoglobinization under NEAA insufficiency (Figure S3J), indicating that a primary iron defect is not a major regulatory mechanism in maturing red blood cells downstream of LAT3. Although mTORC1 inhibition can block mitochondrial biogenesis (79), we did not find reduced mitochondrial function in cells expressing *Lat3* shRNAs as suggested by lack of changes in mitochondrial proteins (Figure 3A), MitoTracker staining (Figure S3A), and glycolytic and TCA cycle intermediates (Figures S3B and C). Together, these results suggest that α/β-globin protein translational regulation is the principle mechanism that is engaged in erythroid cells to maintain NEAA homeostasis. Translational regulation offers the advantage of a rapid response (20) and is particularly beneficial since maturing erythroid cells become incapable of eliciting transcriptional adaptive responses, such as increased NFE2L1-mediated proteasome degradation (29) after chromatin condensation and enucleation.

The translation of α/β-globin proteins is tightly controlled by heme-regulated eIF2α kinase (HRI) which phosphorylates and inhibits eIF2α when heme is scarce (34). eIF2α is also phosphorylated under severe amino acid depleted conditions by GCN2 (18), raising the possibility that diminished LAT3-mediated transport could influence hemoglobin production through GCN2-eIF2α signaling. However, we did not find an increase in the phosphorylation of Ser[51] in eIF2α in *Lat3* knockdown cells or *lat3a* zebrafish morphants (Figures S4C and D). LAT3 inhibition likely did not sufficiently deplete intracellular NEAAs for uncharged tRNAs to activate GCN2 (15–17). This observation also suggests that

mTORC2 activity is unaffected by LAT3 inhibition since Torc2 stimulates Gcn2 activity in response to amino acid starvation in yeast (80). Instead, our data shows that the coordinate regulation of α/β-globin protein translation in response to NEAA availability involves the mTORC1/4E-BP signaling mechanism which is distinct from the eIF2α-dependent pathway (Figure 7).

Current efforts to identify direct translational targets of mTORC1 have relied upon using pharmacologic mTORC1 inhibitors (27, 28, 32). However, these analyses do not account for homeostatic feedback regulation that can influence the duration, magnitude, and specificity of the response (33, 75). Regulation of α/β-globin protein translation by HRI-eIF2α signalling in which specificity is dictated by heme availability exemplifies the importance of these considerations (34, 81) and highlights how upstream signals can substantially impact downstream translational control. In support of this notion, our polysome-profiling experiments demonstrated that while acute torin 1 treatment markedly blocked translation initiation of multiple proteins (Figure 5D), *Lat3* knockdown had a more selective effect on globin protein translation (Figure 3F). Genes that had TOP-like sequences that are responsive to torin 1 such as *Ybx1* (28) were refractory to LAT3 inhibition (Figure 3F) but remained responsive to torin 1 (Figure 5D). Our findings are consistent with the failure of *Lat1*$^{-/-}$ naïve T-cells to activate due to a selective inability to increase Myc protein abundance (7) and contrasts with the much more severe developmental defects that occur with genetic abrogation of mTORC1 (82–84).

Tissue specificity also likely plays a crucial role in determining mTORC1 translational targets. For example, although vimentin translation is directly regulated by mTORC1 (27, 28), it is not transcriptionally expressed in maturing erythroid cells (85, 86). Currently, tissue-specific transcription start sites remains poorly annotated and likely explains why the dbTSS has no data pertaining to *α/β-globin* mRNAs. The transcriptional programs in different cell types undoubtedly affect translational regulation, and although the use of potent mTORC1 inhibitors has provided considerable insight into mTORC1 translational control, a better understanding of these mechanisms in normal physiology and nutrient homeostasis is needed.

Our work has broad clinical implications. Clinical use of mTOR inhibitors has been associated with pronounced microcytic anemia, leukopenia, and thrombocytopenia in humans (87, 88). Some of these symptoms may be the result of defective hematopoietic stem cell function where mTORC1 activity and proper translational regulation are essential (82, 89, 90). However, our work suggests that these processes are also critical in committed erythroid cells, and the future clinical use of mTORC1 inhibitors with greater efficacy at blocking mTORC1-mediated translation is likely to cause a higher incidence of anemias. Our results also are an example of how a better understanding of amino acid metabolism positively impacts human health by providing an explanation as to why modulation of the mTORC1 pathway has been successful in treating human blood disorders. Rapamycin improves thalassemia symptoms in a murine model (91), and our data suggests that this effect is due to inhibition of defective globin translation, thereby correcting the globin chain imbalance and decreasing the formation of toxic aggregates. Conversely, L-leucine administration rescues several defects associated with DBA in animal models, cultured

human CD34^{+} hematopoietic progenitors, as well as a human DBA patient (39, 92–95) and has led to ongoing multicenter clinical trials (in Phase 1 and 2) to assess the therapeutic benefits of L-leucine in the treatment of transfusion-dependent DBA patients. Although it is tempting to speculate that defective L-leucine or NEAA metabolism plays an etiological role in the actual development of DBAs or other human diseases arising from aberrant protein translation such as autism and Robert's Syndromes cohesinopathies, whether this is truly the case is currently unknown (1–4, 37). Thus, further work directed at unravelling amino acid metabolism may not only uncover new causes of human disease but also lead to more mainstream use of amino acid supplementation as an effective treatment modality for a broad range of disorders.

Materials and Methods

Cell culture

Friend murine erythroleukemia (MEL) DS19 cells were cultured and differentiated with 2% DMSO as previously described (47). Primary fetal liver cells were harvested from E13.5 CD1 embryos. Following dissections, livers were washed once with HBSS. Cells were dissociated and maintained in culture media consisting of StemPro-34 media and supplement (Gibco, Carlsbad, CA, USA), 100 U/mL penicillin, 100 μg/mL streptomycin, 2 mM L-glutamine, and freshly added 0.5 U/mL erythropoietin, 100 ng/mL stem cell factor, and 1 μM dexamethasone.

DS19 MEL cells were treated with 1 μM rapamycin (LC Laboratories, Woburn, MA, USA) for twenty-four hours or four days, 100 nM torin 1 (Tocris, Bristol, UK), 50 μM 4EGI-1 (Millipore, Billerica, MA, USA), 1 μM DG2 (Millipore), 10 μM chlororquine, or 10 mM 2-aminobicyclo-(2,2,1)-heptane-2-carboxylic acid (BCH) (Sigma-Aldrich, St. Louis, MO, USA) for four days and o-dianisidine stained as described below. Amino acid esters were added to cells at a concentration of 0.8 mM (Sigma-Aldrich for all amino acid esters except for isoleucine-ester, which was purchased from VWR (Radnor, PA, USA)).

MEL cells were electroporated with NT9 (Control) or two shRNAs targeting *Lat3* (shRNA-1 and shRNA-2) and cultured in media containing 5 μg/mL puromycin as previously described (47).

Three days after isolation, fetal liver cells were infected with lentiviruses expressing either a control shRNA or shRNA targeting murine *Lat3*. Two days after infection, cells were switched to differentiation medium consisting of StemPro-34 + supplement, 100 U/mL penicillin, 100 μg/mL streptomycin, 2 mM L-glutamine, and freshly added 5 U/mL erythropoietin, 1 mg/mL holo-transferrin, and 0.4 U/μL insulin and incubated for another two days at 37°C. Cells were then o-dianisidine stained to determine the extent of hemoglobinization.

Human CD34^{+} cells from mobilized peripheral blood of healthy donors were obtained from the Center of Excellence in Molecular Hematology at Fred Hutchinson Cancer Research Center, Seattle, Washington. After thawing, 10^6 cells maintained in stem cell media (SFEM supplemented with 100 ng/mL Flt3L and 10 ng/mL hTPO) for two days to recover. Stem

cell media was a generous gift of Dr. Benjamin Ebert (Harvard Medical School, Boston, MA). Cells were then switched to erythroid differentiation media (SFEM supplemented with 2 mM L-glutamine, 100 U/mL penicillin, 100 μg/mL streptomycin,, 1 mg/mL holo-transferrin, 10 μM β-mercaptoethanol, 4 μg/mL dexamethasone, 25 ng/mL rhSCF, and 0.5 U/mL hEpo. After 7 days, total RNA was isolated.

Zebrafish experiments

All zebrafish experiments were performed in accordance with IACUC regulations. Injections and *in situ* hybridizations were performed as previously described (47, 53). Quantification by flow cytometry using fluorescently labeled transgenic zebrafish embryos was performed as previously described (96, 97). Morpholinos were purchased from Gene Tools, LLC (Philomath, OR, USA).

Zebrafish embryos at the one-cell stage were injected with morpholinos (MOs). The sequence of the morpholinos targeting the exon 4-intron 4 (MO1) and the exon 5-intron 5 (MO2) of *D. rerio lat3a* (please see "Bioinformatic and statistical analysis" for accession numbers) were as follows: *lat3a* MO1: 5′-ATAGATCATGTACTCACCTTCTGGT-3′; *lat3a* MO2: 5′-CATTTTCTGCTGCTCCTTACCGTTA-3′. The MO targeting zebrafish *lat1* (NM_001128358) at the exon 1-intron 1 boundary was 5′-AGGTAACAGTTTACTTACGTATACA-3′.

Zebrafish embryos at 19 hpf (20 somites) were chemically dechorionated with pronase (Roche, Basel, Switzerland) and treated with DMSO (vehicle), 50 μM rapamycin, 1 μM torin 1, or 10 μM 4EGI-1 and *o*-dianisidine stained at 72 hpf (96).

Quantitative and semi-quantitative RT-PCR

RT-PCRs were performed as previously described with modifications (47). Total RNA was isolated from cells or 72 hpf zebrafish embryos using the Qiagen (Hilden, Germany) RNeasy Plus Mini Kit with on-column DNase digestion with the RNase-free DNase set (Qiagen) according to the manufacturer's instructions.

o-dianisidine and trypan blue staining and cell proliferation

o-dianisidine staining of MEL cells and zebrafish embryos were performed as described elsewhere (47). Trypan blue staining was performed according to the manufacturer's instructions (Gibco) on day 4 differentiated control or shRNA expressing MEL cells. For cell proliferation, control or MEL cells expressing *Lat3* shRNAs were counted on days 0 to 4 of DMSO differentiation.

Metabolic labeling

^{55}Fe-transferrin (^{55}FeCl$_3$, specific activity = 54.5 mCi/mol, Perkin Elmer, Waltham, MA, USA) metabolic labeling was performed as previously described (47, 98). [^{3}H]-L-leucine labeling was performed as described elsewhere with modifications (7). Two million cells were resuspended in 1 mL of leucine-free media (Crystalgen, Commack, NW, USA) supplemented with 10% dialyzed fetal bovine serum (Invitrogen, Carlsbad, CA, USA), 0.5 mCi/mL of [^{3}H]-L-leucine (specific activity = 106.2 Ci/mmol, Perkin Elmer) and incubated

for 4 minutes at 37°C. Competition assays were performed in the presence of 10 mM BCH or the indicated amino acids (Sigma-Aldrich). Cells were then washed twice with PBS and resuspended in 500 μL of PBS and radioactivity was measured by liquid scintillation.

Non-radioactive metabolic labeling was performed using the Click-iT kit Protein Reaction Buffer Kit (Molecular Probes, Eugene, OR, USA) with Click-iT L-azidohomoalanine (L-AHA) (Molecular Probes) and biotin alkyne (Molecular Probes) according to the manufacturer's instructions. Non-radioactive metabolic labeling of shRNA expressing cells was carried out for four hours. For experiments involving acute treatment with torin 1, cells were first pre-treated for 30 minutes with 250 nM torin 1, washed with PBS, and subsequently labeled for one hour in cysteine/methionine-free media (Gibco) supplemented with 10% dialyzed fetal bovine serum, 2 mM L-glutamine, 1 mM sodium pyruvate, 50 μM L-AHA, 2% DMSO, and 250 nM torin 1 for an additional two hours at 37°C. BCH experiments were similarly performed except that 10 mM BCH pre-treatment was for one hour. Esterified amino acids were added to the cells at the same time as pre-treatment and regular treatment at a concentration of 0.8 mM.

Chloroquine was added to cells at the same time as torin 1 at 1 mM. Labeled lysates were resolved on SDS-PAGE, and analyzed by chemiluminescence using streptavidin-horseradish peroxidase (ThermoFisher Scientific, Waltham, MA, USA) and western blotting.

Lentivirus production and infection

Lentiviruses were produced as previously described with the following changes (99). HEK 293T cells were transfected with plasmids encoding psPax2, VSV-G, and various shRNAs using ProFection Calcium Phosphate Kit (Promega, Madison, WI, USA) according to the manufacturer's instructions. One day after transfection, media was changed to low-serum media (5%) and incubated at 37°C for another two days. Cell culture media supernatant was collected and centrifuged at 24,000 rpm for two hours. The viral pellet was resuspended in 200 μL of DMEM. To infect cells, 50 μL of virus was added to the cells.

shRNAs and the NT9 control in a pLKO.1-puro vector backbone were purchased from Sigma-Alrich. The sequences of hairpin shRNAs were as follows: for *Lat3* shRNA-1, 5′-CCGGCCCTGGAATCAAGCTGATCTACTCGAGTAGATCAGCTTGATTCCAGGGTT TTTG-3′; for *Lat3* shRNA-2, 5′-CCGGGCTTCGGGTCATCTTCTATATCTCGAGATATAGAAGATGACCCGAAGCTT TTTG-3′.

In situ hybridizations

In situ hybridization on sectioned murine embryonic tissue and zebrafish embyos were performed as previously described (47, 53).

CRISPR/Cas9-mediated genomic excision of *Eif4ebp1* and *Eif4ebp2*

Eif4ebp1 and *Eif4ebp2* were sequentially deleted in MEL cells as described previously with modifications (100, 101). Briefly, CRISPR guide sequences were designed to direct two cleavages at the *Eif4ebp1* and *Eif4ebp2* loci to generate a chromosomal deletion (101).

CRISPR guide sequences were designed to have a unique 12 nucleotide seed sequence 5′-NNNNNNNNNNNN-NGG-3′ in the mouse genome (http://www.genome-engineering.org) to minimize off-target cleavages. CRISPR guides were cloned into pX330 plasmid (Addgene, Cambridge, MA, USA) with BbsI ligation as previously described (100). Deletion of both genes was performed in a similar manner to previous reports (100–102). The CRISPR oligo sequences were as follows. For *Eif4ebp1*, the 5′ CRISPR oligos were 5′-CACCGTTCTTCTCTGAGGATCGGCC-3′ and 5′-AAACGGCCGATCCTCAGAGAAGAAC-3′, and the 3′ CRISPR oligos were 5′-CACCGTATAAAGGAGAGCGTTTAGC-3′ and 5′-AAACGCTAAACGCTCTCCTTTATAC-3′. For *Eif4ebp2*, the 5′ CRISPR oligos were 5′-CACCGCTACCGGAAGCGGTCGAAGG-3′ and 5′-AAACCCTTCGACCGCTTCCGGTAGC-3′, and the 3′ CRISPR oligos were 5′-CACCGCATGCACACGGCTCCGGTGT-3′ and 5′-AAACACACCGGAGCCGTGTGCATGC-3′.

CRISPR/Cas9 constructs were delivered to MEL cells by electroporation. One million MEL cells were resuspended in BTX solution with 2 μg of each of two CRISPR/Cas9 constructs (which had been designed to generate flanking cleavages resulting in a deletion) and 0.2 μg pmaxGFP (Lonza, Hopkinton, MA, USA), transferred to a 2 mm cuvette and electroporated at 250V and 5 ms using a BTX ECM 830 electroporator (Harvard Apparatus, Holliston, MA, USA). Cells were placed immediately in 5 mL media at 30°C. One to three days later cells were sorted by FACS with gating on the 1–3% brightest GFP-positive live events. Cells were plated by limiting dilution at 0.3 cells per well in 96-well plates and cultured at 37°C. Genomic DNA was isolated from individual clones using QuickExtract (Epicentre, Madison, WI) according to the manufacturer's instructions and were screened by PCR for the wild-type and deletion allele with HotStartTaq DNA Polymerase Kit and confirmed by immunoblot analysis. The primers used for genotyping were as follows. For *Eif4ebp1*, the forward (F) primer was 5′-AGTACGCAGAGCTTCGATCC-3′, the reverse-1 (R1) primer was 5′-GAGTCTGGCTGCAGCTGCTG-3′, and the reverse-2 (R2) primer was 5′-ACCCTCCCTCTCTTCTCCAG-3′. For *Eif4ebp2*, the F primer was 5′-ACCCTCTGCCTCTAGCCTTC-3′, the R1 primer was 5′-CACGCTCGGCTCTCAACTCG-3′, and the R2 primer was 5′-CCACCTTCCTGTGGTAAGGA-3′.

Immunoblotting

Immunoblotting was performed as previously described (99). Anti-LAT3 (ab55552), anti-PDHD (ab67592), and anti-COX-IV (ab16056) rabbit polyclonal antibodies were purchased from Abcam (Cambridge, England). Anti-GAPDH (MAB374) and anti-TFRC (136800) mouse monoclonal antibodies were purchased from Millipore and Invitrogen, respectively. Mouse monoclonal anti-ATP6V1H (G-2), anti-TUBA1A (DM1A), and anti-ACTB (C-2) and goat polyclonal anti-FECH (C-20), anti-HSPD1 (K-19), and anti-GATA1 (N-1) antibodies were purchased from Santa Cruz Biotechnology (Dallas, TX, USA). Rabbit monoclonal anti-LC3B (2775S), anti-(pS51)eIF2α (D9G8), anti-eIF2α (D7D3), anti-(pT37/pT46)4E-BP1 (236B4), anti-(pT389)S6K1 (108D2), anti-4E-BP1 (53H11), anti-4E-BP2 (#2845), anti-S6K1 (49D7), and anti-(pS240/244)S6 (D68F8) and mouse monoclonal anti-

S6 (54D2) were purchased from Cell Signaling Technologies (Danvers, MA, USA). The rabbit polyclonal anti-PPOX antibody was a generous gift of Dr. Harry A. Dailey (University of Georgia, GA, USA). The rabbit polyclonal anti-Ankyrin1 and anti-EPB42 antibodies were generous gifts of Dr. Samuel E. Lux IV (Harvard Medical School, MA, USA). The anti-ALAS2 rabbit polyclonal antibody was a generous gift of Dr. Hiroshi Munakata (Kinki University, Osaka-Sayama, Japan).

Gas chromatography-mass spectrometry (GC-MS)

Twelve million differentiated cells were washed once in PBS and frozen at −80°C. Metabolite extraction and GC-MS was performed at the Metabolomics Core at the University of Utah (Salt Lake City, UT). 360 μL of 90% methanol was added to the cell pellet to give an approximate final concentration of 80% methanol. Samples were incubated for one hour at −20°C followed by centrifugation at 30 000 × g for 10 minutes at −20°C. The supernatant was transferred to a new tube and vacuum dried. GC-MS analysis was performed using a Waters (Milford, MA, USA) GCT Premier mass spectrometer fitted with an Agilent (Santa Clara, CA, USA) 6890 gas chromatograph and a Gerstel (Mulheim an der Ruhr, Germany) MPS2 autosampler. Dried samples were suspended in 40 μL of 40 mg/mL O-methoxyamine hydrochloride in pyridine and incubated for one hour at 30°C. 25 μL of this solution and 10 μL of N-methyl-N-trimethylsilyltrifluoracetamide were added to the autosampler vials and incubated for one hour at 30°C with shaking. 3 μL of fatty acid methyl ester standard solution was added and 1 μL of this final sample was injected to the gas chromatograph inlet in the split mode with the inlet temperature held at 250°C. A 10:1 split ratio was used for analysis. The gas chromatograph had an initial temperature of 95°C for one minute followed by a 40°C/min ramp to 110°C and held for 2 minutes. This was followed by a second 5°C/min ramp to 250°C, a third ramp to 350°C, and then a final hold of 3 minutes. A 30 m Phenomex (Torrance, CA, USA) ZB5-5 MSi column with a 5 m long guard column was employed for chromatographic separation. Helium was used as the carrier gas at 1 mL/min. Data was collected using MassLynx4.1 software (Waters). Metabolites were identified and their peak area was recorded using QuanLynx (Waters). This data was then transferred to an Excel (Microsoft, Redmond, WA, USA) spreadsheet for further data analysis.

Polysome profiling

Polysome profiling was performed as previously described with modifications (103). Briefly, MEL cells expressing control or *Lat3*-specific shRNA (shRNA-1) were differentiated using 2% DMSO. At day 3 of differentiation, cells were harvested by centrifugation and lysed in buffer containing KCl (0.15 M), Tris-Cl (pH 7, 0.010 M), Nonidet P-40 (0.5%), cycloheximide (150 μg/mL), dithiothreitol (0.020 M), $MgCl_2$ (0.010 M), and rRNAsin (100 U/mL). Lysates were diluted in polysome buffer containing Hepes (0.04 M), KCl (0.1 M), $MgCl_2$ (0.005 M), and trisodium citrate (0.002 M), pH 7.4 and treated with polysome detergent by combining 9 volumes lysate, representative of 20 million cells, with one volume polysome detergent and incubating at 4°C with gentle rocking action for 10 minutes. Treated-lysates were gently loaded onto a linear sucrose gradient (15% to 60% ultrapure sucrose in polysome buffer) for polysome analysis. Gradients were centrifuged at 180,000 × *g* at 4°C for 2 hours in a Sorvall TH-641 swinging bucket rotor.

Tubes containing resolved gradients were fractionated using an ISCO gradient fractionator including the Type 11 Optical Unit at approximately one ml/min and collecting fractions at one-minute intervals as they left the optical unit. The optical density at 254 nm from the optical unit was imported into an Agilent Technologies SS420X interface and exported as millivolts by the EZChromeSI software. Thus, the polysome figures are shown as mVolts as a function of time (minutes). The dead time before the start of fraction collection was about 3 min and the final (tenth) fraction collected after 13 min. Fractions were snap-frozen in liquid nitrogen and stored at −80°C until use. Reverse transcription was performed as described above and semi-quantitative PCR was performed using HotStartTaq DNA Polymerase Kit. For drug treatment, differentiating MEL cells were treated on day 3 of differentiation with 250 nM torin 1 or vehicle for 2 hours before harvest, lysis, and polysome analysis. Densitometry analysis was performed by averaging 3 independent experiments using ImageJ software (104). Data was normalized to total RNA collected in all fractions.

Flow cytometry and fluorescent microscopy analysis

Flow cytometry analysis of zebrafish embryos were performed as described elsewhere (47, 96, 97, 105). Fluorescent microscopy analysis was performed on *Tg(rag2:eGFP)* zebrafish embryos at 96 hpf using the Leica (Allendale, NJ, USA) MZ TLIII microscope and a Leica DC500 camera. Phase contrast and fluorescent images were merged using Adobe Photoshop CS3 (San Jose, CA, USA).

To examine mitochondrial mass, cells were stained with 200 nM of MitoTracker Red 580 (Molecular Probes) according to the manufacturer's instructions. Flow cytometry was performed on the BD FACSCanto II (BD Biosciences, Franklin Lakes, NJ, USA) using the BD FACSDiva Software (BD Biosciences). For analysis of erythroid differentiation and viability, primary murine fetal liver cells were simultaneously stained with APC-conjugated c-KIT and PE-conjugated TER119 antibodies (BD Biosciences) followed by annexin V (BD Biosciences) and 7-AAD (BD Biosciences) staining to measure cell viability. Flow cytometry was carried out on a BD LSRII Flow Cytometer (BD Biosciences) and data analysis was performed using FACSDiva software.

Quantitative and semi-quantitative RT-PCR

PCRs were performed as previously described with modifications (47, 97). Total RNA was isolated from cells or 72 hpf zebrafish embryos using the Qiagen (Hilden, Germany) RNeasy Plus Mini Kit with on-column DNase digestion with the RNase-free DNase set (Qiagen) according to the manufacturer's instructions. One microgram of total RNA was used for reverse transcription with the High Capacity cDNA Reverse Transcription Kit (Applied Biosystems, Carlsbad, CA, USA). Quantitative RT-PCR was performed using gene and species-specific TaqMan probes (Applied Biosystems) or the *α/β-globin* and *Hprt* primers listed below. Semi-quantitative RT-PCR expression and polysome profiling analyses were carried out using FastStart Taq DNA Polymerase (Roche) and HotStartTaq DNA Polymerase Kit (Qiagen), respectively, with the following primers specific for murine genes: for *α-globin*, 5′-TGGCTAGCCAAGGTCACCAGC-3′ and 5′-CTCTCTGGGAAGACAAAAGCAAC-3′; for *βmajor globin*, 5′-

GGTTTAGTGGTACTTGTGAGCC-3′ and 5′-ATGGTGCACCTGACTGATGCTG-3′; and for *Hprt*, 5′-CACAGGACTAGAACACCTGC-3′ and 5′-GCTGGTGAAAAGGACCTCT-3′. All other primers were as previously described (28). Primers specific for zebrafish genes were as follows: for *lat1*, 5′-TGAAACTGTGGATCGAGCTG-3′ and 5′-AGGCATCTTGAACCCTTGTG-3′; for *β-actin* 5′-ACCAGAGGCATACAGGGACAG-3′ and 5′-GTTGGTATGGGACAGAAAGAC-3′.

Bioinformatic and statistical analysis

Analysis of primary fetal liver RNAseq data based upon TER119 and CD71 expression was performed as previously described (45, 47). The accession number for the RNAseq dataset is GSE32110 (www.ncbi.nlm.nih.gov/geo/query/acc.cgi?acc=GSE32110) (45). Amino acid composition was calculated using Expasy (www.expasy.org) and plotted as a heat map using MultiExperiment Viewer (Boston, MA, USA). Phylogenetic analysis of *Lat3* isoforms of various species was performed as previously described (53). The accession numbers of the genes are as follows: *H. sapiens*: NM_003627; *P. troglodytes*: XM_003318000; *M. musculus:* NM_024497; *D. rerio* (*lat3a*): NM_199897; *D. rerio* (*lat3b*): NM_001083000.

The transcription start sites of murine and human *α/β-globin* transcripts were analyzed using sequences from RefSeq, EMSEMBL, and UCSC databases. The most common TSS was compared to consensus sequences defined by previous studies (27, 28).

Student's t-test was used for all statistical analysis except for amino acid competition assay (Figure 1I) where a two-way ANOVA was used.

Supplementary Material

Refer to Web version on PubMed Central for supplementary material.

Acknowledgments

References and Notes

1. Bose T, Lee KK, Lu S, Xu B, Harris B, Slaughter B, Unruh J, Garrett A, McDowell W, Box A, Li H, Peak A, Ramachandran S, Seidel C, Gerton JL. Cohesin proteins promote ribosomal RNA production and protein translation in yeast and human cells. PLoS Genet. 2012; 8:e1002749.10.1371/journal.pgen.1002749 [PubMed: 22719263]

2. Kelleher RJ 3rd, Bear MF. The autistic neuron: troubled translation? Cell. 2008; 135:401–406. published online EpubOct 31. 10.1016/j.cell.2008.10.017 [PubMed: 18984149]

3. Sheen JH, Zoncu R, Kim D, Sabatini DM. Defective regulation of autophagy upon leucine deprivation reveals a targetable liability of human melanoma cells in vitro and in vivo. Cancer cell. 2011; 19:613–628. published online EpubMay 17. 10.1016/j.ccr.2011.03.012 [PubMed: 21575862]

4. Xu B, Lee KK, Zhang L, Gerton JL. Stimulation of mTORC1 with L-leucine rescues defects associated with Roberts syndrome. PLoS Genet. 2013; 9:e1003857.10.1371/journal.pgen.1003857 [PubMed: 24098154]

5. Payne SH, Loomis WF. Retention and loss of amino acid biosynthetic pathways based on analysis of whole-genome sequences. Eukaryotic cell. 2006; 5:272–276. published online EpubFeb. 10.1128/EC.5.2.272-276.2006 [PubMed: 16467468]

6. Broer S. Amino acid transport across mammalian intestinal and renal epithelia. Physiological reviews. 2008; 88:249–286. published online EpubJan. 10.1152/physrev.00018.2006 [PubMed: 18195088]

7. Sinclair LV, Rolf J, Emslie E, Shi YB, Taylor PM, Cantrell DA. Control of amino-acid transport by antigen receptors coordinates the metabolic reprogramming essential for T cell differentiation. Nature immunology. 2013; 14:500–508. published online EpubMay. 10.1038/ni.2556 [PubMed: 23525088]

8. Oxender DL, Christensen HN. Distinct Mediating Systems for the Transport of Neutral Amino Acids by the Ehrlich Cell. J Biol Chem. 1963; 238:3686–3699. published online EpubNov. [PubMed: 14109206]

9. Babu E, Kanai Y, Chairoungdua A, Kim DK, Iribe Y, Tangtrongsup S, Jutabha P, Li Y, Ahmed N, Sakamoto S, Anzai N, Nagamori S, Endou H. Identification of a novel system L amino acid transporter structurally distinct from heterodimeric amino acid transporters. J Biol Chem. 2003; 278:43838–43845. published online EpubOct 31. 10.1074/jbc.M305221200 [PubMed: 12930836]

10. Bodoy S, Martin L, Zorzano A, Palacin M, Estevez R, Bertran J. Identification of LAT4, a novel amino acid transporter with system L activity. J Biol Chem. 2005; 280:12002–12011. published online EpubMar 25. 10.1074/jbc.M408638200 [PubMed: 15659399]

11. Elorza A, Soro-Arnaiz I, Melendez-Rodriguez F, Rodriguez-Vaello V, Marsboom G, de Carcer G, Acosta-Iborra B, Albacete-Albacete L, Ordonez A, Serrano-Oviedo L, Gimenez-Bachs JM, Vara-Vega A, Salinas A, Sanchez-Prieto R, Martin del Rio R, Sanchez-Madrid F, Malumbres M, Landazuri MO, Aragones J. HIF2alpha acts as an mTORC1 activator through the amino acid carrier SLC7A5. Molecular cell. 2012; 48:681–691. published online EpubDec 14. 10.1016/j.molcel.2012.09.017 [PubMed: 23103253]

12. Nicklin P, Bergman P, Zhang B, Triantafellow E, Wang H, Nyfeler B, Yang H, Hild M, Kung C, Wilson C, Myer VE, MacKeigan JP, Porter JA, Wang YK, Cantley LC, Finan PM, Murphy LO. Bidirectional transport of amino acids regulates mTOR and autophagy. Cell. 2009; 136:521–534. published online EpubFeb 6. 10.1016/j.cell.2008.11.044 [PubMed: 19203585]

13. Wang Q, Bailey CG, Ng C, Tiffen J, Thoeng A, Minhas V, Lehman ML, Hendy SC, Buchanan G, Nelson CC, Rasko JE, Holst J. Androgen receptor and nutrient signaling pathways coordinate the demand for increased amino acid transport during prostate cancer progression. Cancer research. 2011; 71:7525–7536. published online EpubDec 15. 10.1158/0008-5472.CAN-11-1821 [PubMed: 22007000]

14. Cohen A, Hall MN. An amino acid shuffle activates mTORC1. Cell. 2009; 136:399–400. published online EpubFeb 6. 10.1016/j.cell.2009.01.021 [PubMed: 19203575]

15. Harding HP, Novoa I, Zhang Y, Zeng H, Wek R, Schapira M, Ron D. Regulated translation initiation controls stress-induced gene expression in mammalian cells. Molecular cell. 2000; 6:1099–1108. published online EpubNov. [PubMed: 11106749]

16. Mueller PP, Hinnebusch AG. Multiple upstream AUG codons mediate translational control of GCN4. Cell. 1986; 45:201–207. published online EpubApr 25. [PubMed: 3516411]

17. Dong J, Qiu H, Garcia-Barrio M, Anderson J, Hinnebusch AG. Uncharged tRNA activates GCN2 by displacing the protein kinase moiety from a bipartite tRNA-binding domain. Molecular cell. 2000; 6:269–279. published online EpubAug. [PubMed: 10983975]

18. Zhang P, McGrath BC, Reinert J, Olsen DS, Lei L, Gill S, Wek SA, Vattem KM, Wek RC, Kimball SR, Jefferson LS, Cavener DR. The GCN2 eIF2alpha kinase is required for adaptation to amino acid deprivation in mice. Mol Cell Biol. 2002; 22:6681–6688. published online EpubOct. [PubMed: 12215525]

19. Ye J, Kumanova M, Hart LS, Sloane K, Zhang H, De Panis DN, Bobrovnikova-Marjon E, Diehl JA, Ron D, Koumenis C. The GCN2-ATF4 pathway is critical for tumour cell survival and proliferation in response to nutrient deprivation. EMBO J. 2010; 29:2082–2096. published online EpubJun 16. 10.1038/emboj.2010.81 [PubMed: 20473272]

20. Sonenberg N, Hinnebusch AG. Regulation of translation initiation in eukaryotes: mechanisms and biological targets. Cell. 2009; 136:731–745. published online EpubFeb 20. 10.1016/j.cell. 2009.01.042 [PubMed: 19239892]

21. Hinnebusch AG. Evidence for translational regulation of the activator of general amino acid control in yeast. Proc Natl Acad Sci U S A. 1984; 81:6442–6446. published online EpubOct. [PubMed: 6387704]

22. Vattem KM, Wek RC. Reinitiation involving upstream ORFs regulates ATF4 mRNA translation in mammalian cells. Proc Natl Acad Sci U S A. 2004; 101:11269–11274. published online EpubAug 3. 10.1073/pnas.0400541101 [PubMed: 15277680]

23. Harding HP, Zhang Y, Zeng H, Novoa I, Lu PD, Calfon M, Sadri N, Yun C, Popko B, Paules R, Stojdl DF, Bell JC, Hettmann T, Leiden JM, Ron D. An integrated stress response regulates amino acid metabolism and resistance to oxidative stress. Molecular cell. 2003; 11:619–633. published online EpubMar. [PubMed: 12667446]

24. Dibble CC, Manning BD. Signal integration by mTORC1 coordinates nutrient input with biosynthetic output. Nature cell biology. 2013; 15:555–564. published online EpubJun. 10.1038/ ncb2763

25. Jewell JL, Russell RC, Guan KL. Amino acid signalling upstream of mTOR. Nature reviews Molecular cell biology. 2013; 14:133–139. published online EpubMar. 10.1038/nrm3522

26. Laplante M, Sabatini DM. mTOR signaling in growth control and disease. Cell. 2012; 149:274–293. published online EpubApr 13. 10.1016/j.cell.2012.03.017 [PubMed: 22500797]

27. Hsieh AC, Liu Y, Edlind MP, Ingolia NT, Janes MR, Sher A, Shi EY, Stumpf CR, Christensen C, Bonham MJ, Wang S, Ren P, Martin M, Jessen K, Feldman ME, Weissman JS, Shokat KM, Rommel C, Ruggero D. The translational landscape of mTOR signalling steers cancer initiation and metastasis. Nature. 2012; 485:55–61. published online EpubMay 3. 10.1038/nature10912 [PubMed: 22367541]

28. Thoreen CC, Chantranupong L, Keys HR, Wang T, Gray NS, Sabatini DM. A unifying model for mTORC1-mediated regulation of mRNA translation. Nature. 2012; 485:109–113. published online EpubMay 3. 10.1038/nature11083 [PubMed: 22552098]

29. Zhang Y, Nicholatos J, Dreier JR, Ricoult SJ, Widenmaier SB, Hotamisligil GS, Kwiatkowski DJ, Manning BD. Coordinated regulation of protein synthesis and degradation by mTORC1. Nature. 2014; 513:440–443. published online EpubSep 18. 10.1038/nature13492 [PubMed: 25043031]

30. Han JM, Jeong SJ, Park MC, Kim G, Kwon NH, Kim HK, Ha SH, Ryu SH, Kim S. Leucyl-tRNA synthetase is an intracellular leucine sensor for the mTORC1-signaling pathway. Cell. 2012; 149:410–424. published online EpubApr 13. 10.1016/j.cell.2012.02.044 [PubMed: 22424946]

31. Bonfils G, Jaquenoud M, Bontron S, Ostrowicz C, Ungermann C, De Virgilio C. Leucyl-tRNA synthetase controls TORC1 via the EGO complex. Molecular cell. 2012; 46:105–110. published online EpubApr 13. 10.1016/j.molcel.2012.02.009 [PubMed: 22424774]

32. Larsson O, Morita M, Topisirovic I, Alain T, Blouin MJ, Pollak M, Sonenberg N. Distinct perturbation of the translatome by the antidiabetic drug metformin. Proc Natl Acad Sci U S A. 2012; 109:8977–8982. published online EpubJun 5. 10.1073/pnas.1201689109 [PubMed: 22611195]

33. Ma XM, Blenis J. Molecular mechanisms of mTOR-mediated translational control. Nature reviews Molecular cell biology. 2009; 10:307–318. published online EpubMay. 10.1038/nrm2672

34. Han AP, Yu C, Lu L, Fujiwara Y, Browne C, Chin G, Fleming M, Leboulch P, Orkin SH, Chen JJ. Heme-regulated eIF2alpha kinase (HRI) is required for translational regulation and survival of erythroid precursors in iron deficiency. EMBO J. 2001; 20:6909–6918. published online EpubDec 3. 10.1093/emboj/20.23.6909 [PubMed: 11726526]

35. D'Amici GM, Rinalducci S, Zolla L. Depletion of hemoglobin and carbonic anhydrase from erythrocyte cytosolic samples by preparative clear native electrophoresis. Nature protocols. 2012; 7:36–44. published online EpubJan. 10.1038/nprot.2011.427

36. Quarello P, Garelli E, Brusco A, Carando A, Mancini C, Pappi P, Vinti L, Svahn J, Dianzani I, Ramenghi U. High frequency of ribosomal protein gene deletions in Italian Diamond-Blackfan anemia patients detected by multiplex ligation-dependent probe amplification assay. Haematologica. 2012; 97:1813–1817. published online EpubDec. 10.3324/haematol.2012.062281 [PubMed: 22689679]

37. Ludwig LS, Gazda HT, Eng JC, Eichhorn SW, Thiru P, Ghazvinian R, George TI, Gotlib JR, Beggs AH, Sieff CA, Lodish HF, Lander ES, Sankaran VG. Altered translation of GATA1 in Diamond-Blackfan anemia. Nature medicine. 2014; 20:748–753. published online EpubJul. 10.1038/nm.3557

38. Ruggero D, Shimamura A. Marrow failure: a window into ribosome biology. Blood. 2014; 124:2784–2792. published online EpubOct 30. 10.1182/blood-2014-04-526301 [PubMed: 25237201]

39. Payne EM, Virgilio M, Narla A, Sun H, Levine M, Paw BH, Berliner N, Look AT, Ebert BL, Khanna-Gupta A. L-Leucine improves the anemia and developmental defects associated with Diamond-Blackfan anemia and del(5q) MDS by activating the mTOR pathway. Blood. 2012; 120:2214–2224. published online EpubSep 13. 10.1182/blood-2011-10-382986 [PubMed: 22734070]

40. Isern J, He Z, Fraser ST, Nowotschin S, Ferrer-Vaquer A, Moore R, Hadjantonakis AK, Schulz V, Tuck D, Gallagher PG, Baron MH. Single-lineage transcriptome analysis reveals key regulatory pathways in primitive erythroid progenitors in the mouse embryo. Blood. 2011; 117:4924–4934. published online EpubMay 5. 10.1182/blood-2010-10-313676 [PubMed: 21263157]

41. Sandoval H, Thiagarajan P, Dasgupta SK, Schumacher A, Prchal JT, Chen M, Wang J. Essential role for Nix in autophagic maturation of erythroid cells. Nature. 2008; 454:232–235. published online EpubJul 10. 10.1038/nature07006 [PubMed: 18454133]

42. Hattangadi SM, Martinez-Morilla S, Patterson HC, Shi J, Burke K, Avila-Figueroa A, Venkatesan S, Wang J, Paulsen K, Gorlich D, Murata-Hori M, Lodish HF. Histones to the cytosol: Exportin 7 is essential for normal terminal erythroid nuclear maturation. Blood. 2014 published online EpubAug 4. 10.1182/blood-2013-11-537761

43. Schweers RL, Zhang J, Randall MS, Loyd MR, Li W, Dorsey FC, Kundu M, Opferman JT, Cleveland JL, Miller JL, Ney PA. NIX is required for programmed mitochondrial clearance during reticulocyte maturation. Proc Natl Acad Sci U S A. 2007; 104:19500–19505. published online EpubDec 4. 10.1073/pnas.0708818104 [PubMed: 18048346]

44. Zhang J, Socolovsky M, Gross AW, Lodish HF. Role of Ras signaling in erythroid differentiation of mouse fetal liver cells: functional analysis by a flow cytometry-based novel culture system. Blood. 2003; 102:3938–3946. published online EpubDec 1 (10.1182/blood-2003-05-1479 2003-05-1479 [pii]). [PubMed: 12907435]

45. Wong P, Hattangadi SM, Cheng AW, Frampton GM, Young RA, Lodish HF. Gene induction and repression during terminal erythropoiesis are mediated by distinct epigenetic changes. Blood. 2011; 118:e128–138. published online EpubOct 20. 10.1182/blood-2011-03-341404 [PubMed: 21860024]

46. Yien YY, Robledo RF, Schultz IJ, Takahashi-Makise N, Gwynn B, Bauer DE, Dass A, Yi G, Li L, Hildick-Smith GJ, Cooney JD, Pierce EL, Mohler K, Dailey TA, Miyata N, Kingsley PD, Garone C, Hattangadi SM, Huang H, Chen W, Keenan EM, Shah DI, Schlaeger TM, DiMauro S, Orkin SH, Cantor AB, Palis J, Koehler CM, Lodish HF, Kaplan J, Ward DM, Dailey HA, Phillips JD, Peters LL, Paw BH. TMEM14C is required for erythroid mitochondrial heme metabolism. J Clin

Invest. 2014; 124:4294–4304. published online EpubOct 1. 10.1172/JCI76979 [PubMed: 25157825]

47. Chen C, Garcia-Santos D, Ishikawa Y, Seguin A, Li L, Fegan KH, Hildick-Smith GJ, Shah DI, Cooney JD, Chen W, King MJ, Yien YY, Schultz IJ, Anderson H, Dalton AJ, Freedman ML, Kingsley PD, Palis J, Hattangadi SM, Lodish HF, Ward DM, Kaplan J, Maeda T, Ponka P, Paw BH. Snx3 regulates recycling of the transferrin receptor and iron assimilation. Cell Metab. 2013; 17:343–352. published online EpubMar 5. 10.1016/j.cmet.2013.01.013 [PubMed: 23416069]

48. Ney PA, D'Andrea AD. Friend erythroleukemia revisited. Blood. 2000; 96:3675–3680. published online EpubDec 1. [PubMed: 11090047]

49. Yu M, Riva L, Xie H, Schindler Y, Moran TB, Cheng Y, Yu D, Hardison R, Weiss MJ, Orkin SH, Bernstein BE, Fraenkel E, Cantor AB. Insights into GATA-1-mediated gene activation versus repression via genome-wide chromatin occupancy analysis. Molecular cell. 2009; 36:682–695. published online EpubNov 25. 10.1016/j.molcel.2009.11.002 [PubMed: 19941827]

50. Pilon AM, Ajay SS, Kumar SA, Steiner LA, Cherukuri PF, Wincovitch S, Anderson SM, Center NCS, Mullikin JC, Gallagher PG, Hardison RC, Margulies EH, Bodine DM. Genome-wide ChIP-Seq reveals a dramatic shift in the binding of the transcription factor erythroid Kruppel-like factor during erythrocyte differentiation. Blood. 2011; 118:e139–148. published online EpubOct 27. 10.1182/blood-2011-05-355107 [PubMed: 21900194]

51. Tallack MR, Magor GW, Dartigues B, Sun L, Huang S, Fittock JM, Fry SV, Glazov EA, Bailey TL, Perkins AC. Novel roles for KLF1 in erythropoiesis revealed by mRNA-seq. Genome research. 2012; 22:2385–2398. published online EpubDec. 10.1101/gr.135707.111 [PubMed: 22835905]

52. Postlethwait JH, Yan YL, Gates MA, Horne S, Amores A, Brownlie A, Donovan A, Egan ES, Force A, Gong Z, Goutel C, Fritz A, Kelsh R, Knapik E, Liao E, Paw B, Ransom D, Singer A, Thomson M, Abduljabbar TS, Yelick P, Beier D, Joly JS, Larhammar D, Rosa F, Westerfield M, Zon LI, Johnson SL, Talbot WS. Vertebrate genome evolution and the zebrafish gene map. Nat Genet. 1998; 18:345–349. published online EpubApr. 10.1038/ng0498-345 [PubMed: 9537416]

53. Shah DI, Takahashi-Makise N, Cooney JD, Li L, Schultz IJ, Pierce EL, Narla A, Seguin A, Hattangadi SM, Medlock AE, Langer NB, Dailey TA, Hurst SN, Faccenda D, Wiwczar JM, Heggers SK, Vogin G, Chen W, Chen C, Campagna DR, Brugnara C, Zhou Y, Ebert BL, Danial NN, Fleming MD, Ward DM, Campanella M, Dailey HA, Kaplan J, Paw BH. Mitochondrial Atpif1 regulates haem synthesis in developing erythroblasts. Nature. 2012; 491:608–612. published online EpubNov 22. 10.1038/nature11536 [PubMed: 23135403]

54. Schulte-Merker S, Lee KJ, McMahon AP, Hammerschmidt M. The zebrafish organizer requires chordino. Nature. 1997; 387:862–863. published online EpubJun 26. 10.1038/43092 [PubMed: 9202118]

55. Griffin KJ, Amacher SL, Kimmel CB, Kimelman D. Molecular identification of spadetail: regulation of zebrafish trunk and tail mesoderm formation by T-box genes. Development. 1998; 125:3379–3388. published online EpubSep. [PubMed: 9693141]

56. Sekine Y, Nishibori Y, Akimoto Y, Kudo A, Ito N, Fukuhara D, Kurayama R, Higashihara E, Babu E, Kanai Y, Asanuma K, Nagata M, Majumdar A, Tryggvason K, Yan K. Amino acid transporter LAT3 is required for podocyte development and function. Journal of the American Society of Nephrology : JASN. 2009; 20:1586–1596. published online EpubJul. 10.1681/ASN. 2008070809 [PubMed: 19443642]

57. Ramos P, Casu C, Gardenghi S, Breda L, Crielaard BJ, Guy E, Marongiu MF, Gupta R, Levine RL, Abdel-Wahab O, Ebert BL, Van Rooijen N, Ghaffari S, Grady RW, Giardina PJ, Rivella S. Macrophages support pathological erythropoiesis in polycythemia vera and beta-thalassemia. Nature medicine. 2013; 19:437–445. published online EpubApr. 10.1038/nm.3126

58. Tallack MR, Keys JR, Humbert PO, Perkins AC. EKLF/KLF1 controls cell cycle entry via direct regulation of E2f2. J Biol Chem. 2009; 284:20966–20974. published online EpubJul 31. 10.1074/jbc.M109.006346 [PubMed: 19457859]

59. Orkin SH, Zon LI. Hematopoiesis: an evolving paradigm for stem cell biology. Cell. 2008; 132:631–644. published online EpubFeb 22. 10.1016/j.cell.2008.01.025 [PubMed: 18295580]

60. Paw BH, Davidson AJ, Zhou Y, Li R, Pratt SJ, Lee C, Trede NS, Brownlie A, Donovan A, Liao EC, Ziai JM, Drejer AH, Guo W, Kim CH, Gwynn B, Peters LL, Chernova MN, Alper SL, Zapata

A, Wickramasinghe SN, Lee MJ, Lux SE, Fritz A, Postlethwait JH, Zon LI. Cell-specific mitotic defect and dyserythropoiesis associated with erythroid band 3 deficiency. Nat Genet. 2003; 34:59–64. published online EpubMay (10.1038/ng1137 ng1137 [pii]). [PubMed: 12669066]

61. Rekhtman N, Radparvar F, Evans T, Skoultchi AI. Direct interaction of hematopoietic transcription factors PU.1 and GATA-1: functional antagonism in erythroid cells. Genes Dev. 1999; 13:1398–1411. published online EpubJun 1. [PubMed: 10364157]

62. Pop R, Shearstone JR, Shen Q, Liu Y, Hallstrom K, Koulnis M, Gribnau J, Socolovsky M. A key commitment step in erythropoiesis is synchronized with the cell cycle clock through mutual inhibition between PU.1 and S-phase progression. PLoS biology. 2010; 810.1371/journal.pbio. 1000484

63. Schultz IJ, Chen C, Paw BH, Hamza I. Iron and porphyrin trafficking in heme biogenesis. J Biol Chem. 2010; 285:26753–26759. published online EpubAug 27 R110.119503 [pii]. 10.1074/jbc.R110.119503 [PubMed: 20522548]

64. Yuan X, Fleming MD, Hamza I. Heme transport and erythropoiesis. Current opinion in chemical biology. 2013; 17:204–211. published online EpubApr. 10.1016/j.cbpa.2013.01.010 [PubMed: 23415705]

65. Khandros E, Thom CS, D'Souza J, Weiss MJ. Integrated protein quality-control pathways regulate free alpha-globin in murine beta-thalassemia. Blood. 2012; 119:5265–5275. published online EpubMay 31. 10.1182/blood-2011-12-397729 [PubMed: 22427201]

66. Ingolia NT. Ribosome profiling: new views of translation, from single codons to genome scale. Nature reviews Genetics. 2014; 15:205–213. published online EpubMar. 10.1038/nrg3645

67. Patterson AD, Hollander MC, Miller GF, Fornace AJ Jr. Gadd34 requirement for normal hemoglobin synthesis. Mol Cell Biol. 2006; 26:1644–1653. published online EpubMar. 10.1128/MCB.26.5.1644-1653.2006 [PubMed: 16478986]

68. Nathan DG, Lodish HF, Kan YW, Housman D. Beta thalassemia and translation of globin messenger RNA. Proc Natl Acad Sci U S A. 1971; 68:2514–2518. published online EpubOct. [PubMed: 5289885]

69. Lodish HF. Model for the regulation of mRNA translation applied to haemoglobin synthesis. Nature. 1974; 251:385–388. published online EpubOct 4. [PubMed: 4421673]

70. Ingolia NT, Ghaemmaghami S, Newman JR, Weissman JS. Genome-wide analysis in vivo of translation with nucleotide resolution using ribosome profiling. Science. 2009; 324:218–223. published online EpubApr 10. 10.1126/science.1168978 [PubMed: 19213877]

71. Redpath NT, Foulstone EJ, Proud CG. Regulation of translation elongation factor-2 by insulin via a rapamycin-sensitive signalling pathway. EMBO J. 1996; 15:2291–2297. published online EpubMay 1. [PubMed: 8641294]

72. Browne GJ, Proud CG. A novel mTOR-regulated phosphorylation site in elongation factor 2 kinase modulates the activity of the kinase and its binding to calmodulin. Mol Cell Biol. 2004; 24:2986–2997. published online EpubApr. [PubMed: 15024086]

73. Zoncu R, Bar-Peled L, Efeyan A, Wang S, Sancak Y, Sabatini DM. mTORC1 senses lysosomal amino acids through an inside-out mechanism that requires the vacuolar H(+)-ATPase. Science. 2011; 334:678–683. published online EpubNov 4. 10.1126/science.1207056 [PubMed: 22053050]

74. Kang SA, Pacold ME, Cervantes CL, Lim D, Lou HJ, Ottina K, Gray NS, Turk BE, Yaffe MB, Sabatini DM. mTORC1 phosphorylation sites encode their sensitivity to starvation and rapamycin. Science. 2013; 341:1236566. published online EpubJul 26. 10.1126/science.1236566 [PubMed: 23888043]

75. Clohessy JG, Reschke M, Pandolfi PP. Found in translation of mTOR signaling. Cell research. 2012; 22:1315–1318. published online EpubSep. 10.1038/cr.2012.85 [PubMed: 22641373]

76. Gkogkas CG, Khoutorsky A, Ran I, Rampakakis E, Nevarko T, Weatherill DB, Vasuta C, Yee S, Truitt M, Dallaire P, Major F, Lasko P, Ruggero D, Nader K, Lacaille JC, Sonenberg N. Autism-related deficits via dysregulated eIF4E-dependent translational control. Nature. 2013; 493:371–377. published online EpubJan 17. 10.1038/nature11628 [PubMed: 23172145]

77. Amaravadi RK, Yu D, Lum JJ, Bui T, Christophorou MA, Evan GI, Thomas-Tikhonenko A, Thompson CB. Autophagy inhibition enhances therapy-induced apoptosis in a Myc-induced

model of lymphoma. J Clin Invest. 2007; 117:326–336. published online EpubFeb. 10.1172/JCI28833 [PubMed: 17235397]

78. Bayeva M, Khechaduri A, Puig S, Chang HC, Patial S, Blackshear PJ, Ardehali H. mTOR regulates cellular iron homeostasis through tristetraprolin. Cell Metab. 2012; 16:645–657. published online EpubNov 7. 10.1016/j.cmet.2012.10.001 [PubMed: 23102618]

79. Morita M, Gravel SP, Chenard V, Sikstrom K, Zheng L, Alain T, Gandin V, Avizonis D, Arguello M, Zakaria C, McLaughlan S, Nouet Y, Pause A, Pollak M, Gottlieb E, Larsson O, St-Pierre J, Topisirovic I, Sonenberg N. mTORC1 Controls Mitochondrial Activity and Biogenesis through 4E-BP-Dependent Translational Regulation. Cell Metab. 2013; 18:698–711. published online EpubNov 5. 10.1016/j.cmet.2013.10.001 [PubMed: 24206664]

80. Vlahakis A, Graef M, Nunnari J, Powers T. TOR complex 2-Ypk1 signaling is an essential positive regulator of the general amino acid control response and autophagy. Proc Natl Acad Sci U S A. 2014; 111:10586–10591. published online EpubJul 22. 10.1073/pnas.1406305111 [PubMed: 25002487]

81. Chen JJ. Regulation of protein synthesis by the heme-regulated eIF2alpha kinase: relevance to anemias. Blood. 2007; 109:2693–2699. published online EpubApr 1. 10.1182/blood-2006-08-041830 [PubMed: 17110456]

82. Kalaitzidis D, Sykes SM, Wang Z, Punt N, Tang Y, Ragu C, Sinha AU, Lane SW, Souza AL, Clish CB, Anastasiou D, Gilliland DG, Scadden DT, Guertin DA, Armstrong SA. mTOR complex 1 plays critical roles in hematopoiesis and Pten-loss-evoked leukemogenesis. Cell stem cell. 2012; 11:429–439. published online EpubSep 7. 10.1016/j.stem.2012.06.009 [PubMed: 22958934]

83. Chen J, Long F. mTORC1 signaling controls mammalian skeletal growth through stimulation of protein synthesis. Development. 2014; 141:2848–2854. published online EpubJul. 10.1242/dev.108811 [PubMed: 24948603]

84. Ka M, Condorelli G, Woodgett JR, Kim WY. mTOR regulates brain morphogenesis by mediating GSK3 signaling. Development. 2014; 141:4076–4086. published online EpubNov. 10.1242/dev.108282 [PubMed: 25273085]

85. Dellagi K, Vainchenker W, Vinci G, Paulin D, Brouet JC. Alteration of vimentin intermediate filament expression during differentiation of human hemopoietic cells. EMBO J. 1983; 2:1509–1514. [PubMed: 11892803]

86. Sangiorgi F, Woods CM, Lazarides E. Vimentin downregulation is an inherent feature of murine erythropoiesis and occurs independently of lineage. Development. 1990; 110:85–96. published online EpubSep. [PubMed: 1706980]

87. Diekmann F, Rovira J, Diaz-Ricart M, Arellano EM, Vodenik B, Jou JM, Vives-Corrons JL, Escolar G, Campistol JM. mTOR inhibition and erythropoiesis: microcytosis or anaemia? Nephrology, dialysis, transplantation : official publication of the European Dialysis and Transplant Association – European Renal Association. 2012; 27:537–541. published online EpubFeb. 10.1093/ndt/gfr318

88. Xu J, Tian D. Hematologic toxicities associated with mTOR inhibitors temsirolimus and everolimus in cancer patients: a systematic review and meta-analysis. Current medical research and opinion. 2014; 30:67–74. published online EpubJan. 10.1185/03007995.2013.844116 [PubMed: 24028709]

89. Signer RA, Magee JA, Salic A, Morrison SJ. Haematopoietic stem cells require a highly regulated protein synthesis rate. Nature. 2014; 509:49–54. published online EpubMay 1. 10.1038/nature13035 [PubMed: 24670665]

90. Zhang Y, Duc AC, Rao S, Sun XL, Bilbee AN, Rhodes M, Li Q, Kappes DJ, Rhodes J, Wiest DL. Control of hematopoietic stem cell emergence by antagonistic functions of ribosomal protein paralogs. Developmental cell. 2013; 24:411–425. published online EpubFeb 25. 10.1016/j.devcel.2013.01.018 [PubMed: 23449473]

91. Camprecios G, Zhang X, D'Escamard V, Rimmele P, Bigarella CL, Izac B, Brugnara C, Bresnick EH, Rivella S, Ghaffari S. Blood. 2012; 120(21) abstract 369.

92. Jaako P, Debnath S, Olsson K, Bryder D, Flygare J, Karlsson S. Dietary L-leucine improves the anemia in a mouse model for Diamond-Blackfan anemia. Blood. 2012; 120:2225–2228. published online EpubSep 13. 10.1182/blood-2012-05-431437 [PubMed: 22791294]

93. Zhang Y, Ear J, Yang Z, Morimoto K, Zhang B, Lin S. Defects of protein production in erythroid cells revealed in a zebrafish Diamond-Blackfan anemia model for mutation in RPS19. Cell death & disease. 2014; 5:e1352.10.1038/cddis.2014.318 [PubMed: 25058426]

94. Narla A, Payne EM, Abayasekara N, Hurst SN, Raiser DM, Look AT, Berliner N, Ebert BL, Khanna-Gupta A. L-Leucine improves the anaemia in models of Diamond Blackfan anaemia and the 5q- syndrome in a TP53-independent way. British journal of haematology. 2014; 167:524–528. published online EpubNov. 10.1111/bjh.13069 [PubMed: 25098371]

95. Pospisilova D, Cmejlova J, Hak J, Adam T, Cmejla R. Successful treatment of a Diamond-Blackfan anemia patient with amino acid leucine. Haematologica. 2007; 92:e66–67. published online EpubMay. [PubMed: 17562599]

96. Cooney JD, Hildick-Smith GJ, Shafizadeh E, McBride PF, Carroll KJ, Anderson H, Shaw GC, Tamplin OJ, Branco DS, Dalton AJ, Shah DI, Wong C, Gallagher PG, Zon LI, North TE, Paw BH. Teleost growth factor independence (gfi) genes differentially regulate successive waves of hematopoiesis. Dev Biol. 2013; 373:431–441. published online EpubJan 15. 10.1016/j.ydbio. 2012.08.015 [PubMed: 22960038]

97. Hildick-Smith GJ, Cooney JD, Garone C, Kremer LS, Haack TB, Thon JN, Miyata N, Lieber DS, Calvo SE, Akman HO, Yien YY, Huston NC, Branco DS, Shah DI, Freedman ML, Koehler CM, Italiano JE Jr, Merkenschlager A, Beblo S, Strom TM, Meitinger T, Freisinger P, Donati MA, Prokisch H, Mootha VK, Dimauro S, Paw BH. Macrocytic anemia and mitochondriopathy resulting from a defect in sideroflexin 4. Am J Hum Genet. 2013; 93:906–914. published online EpubNov 7. 10.1016/j.ajhg.2013.09.011 [PubMed: 24119684]

98. Shaw GC, Cope JJ, Li L, Corson K, Hersey C, Ackermann GE, Gwynn B, Lambert AJ, Wingert RA, Traver D, Trede NS, Barut BA, Zhou Y, Minet E, Donovan A, Brownlie A, Balzan R, Weiss MJ, Peters LL, Kaplan J, Zon LI, Paw BH. Mitoferrin is essential for erythroid iron assimilation. Nature. 2006; 440:96–100. published online EpubMar 2 (nature04512 [pii] 10.1038/nature04512). [PubMed: 16511496]

99. Chung J, Lau J, Cheng LS, Grant RI, Robinson F, Ketela T, Reis PP, Roche O, Kamel-Reid S, Moffat J, Ohh M, Perez-Ordonez B, Kaplan DR, Irwin MS. SATB2 augments DeltaNp63alpha in head and neck squamous cell carcinoma. EMBO reports. 2010; 11:777–783. published online EpubOct. 10.1038/embor.2010.125 [PubMed: 20829881]

100. Bauer DE, Kamran SC, Lessard S, Xu J, Fujiwara Y, Lin C, Shao Z, Canver MC, Smith EC, Pinello L, Sabo PJ, Vierstra J, Voit RA, Yuan GC, Porteus MH, Stamatoyannopoulos JA, Lettre G, Orkin SH. An erythroid enhancer of BCL11A subject to genetic variation determines fetal hemoglobin level. Science. 2013; 342:253–257. published online EpubOct 11. 10.1126/science. 1242088 [PubMed: 24115442]

101. Canver MC, Bauer DE, Dass A, Yien YY, Chung J, Masuda T, Maeda T, Paw BH, Orkin SH. Characterization of genomic deletion efficiency mediated by clustered regularly interspaced palindromic repeats (CRISPR)/Cas9 nuclease system in mammalian cells. J Biol Chem. 2014; 289:21312–21324. published online EpubAug 1. 10.1074/jbc.M114.564625 [PubMed: 24907273]

102. Cong L, Ran FA, Cox D, Lin S, Barretto R, Habib N, Hsu PD, Wu X, Jiang W, Marraffini LA, Zhang F. Multiplex genome engineering using CRISPR/Cas systems. Science. 2013; 339:819–823. published online EpubFeb 15. 10.1126/science.1231143 [PubMed: 23287718]

103. Anderson SA, Nizzi CP, Chang YI, Deck KM, Schmidt PJ, Galy B, Damnernsawad A, Broman AT, Kendziorski C, Hentze MW, Fleming MD, Zhang J, Eisenstein RS. The IRP1-HIF-2alpha axis coordinates iron and oxygen sensing with erythropoiesis and iron absorption. Cell Metab. 2013; 17:282–290. published online EpubFeb 5. 10.1016/j.cmet.2013.01.007 [PubMed: 23395174]

104. Schneider CA, Rasband WS, Eliceiri KW. NIH Image to ImageJ: 25 years of image analysis. Nature methods. 2012; 9:671–675. published online EpubJul. [PubMed: 22930834]

105. Feng H, Stachura DL, White RM, Gutierrez A, Zhang L, Sanda T, Jette CA, Testa JR, Neuberg DS, Langenau DM, Kutok JL, Zon LI, Traver D, Fleming MD, Kanki JP, Look AT. T-lymphoblastic lymphoma cells express high levels of BCL2, S1P1, and ICAM1, leading to a blockade of tumor cell intravasation. Cancer cell. 2010; 18:353–366. published online EpubOct 19. 10.1016/j.ccr.2010.09.009 [PubMed: 20951945]
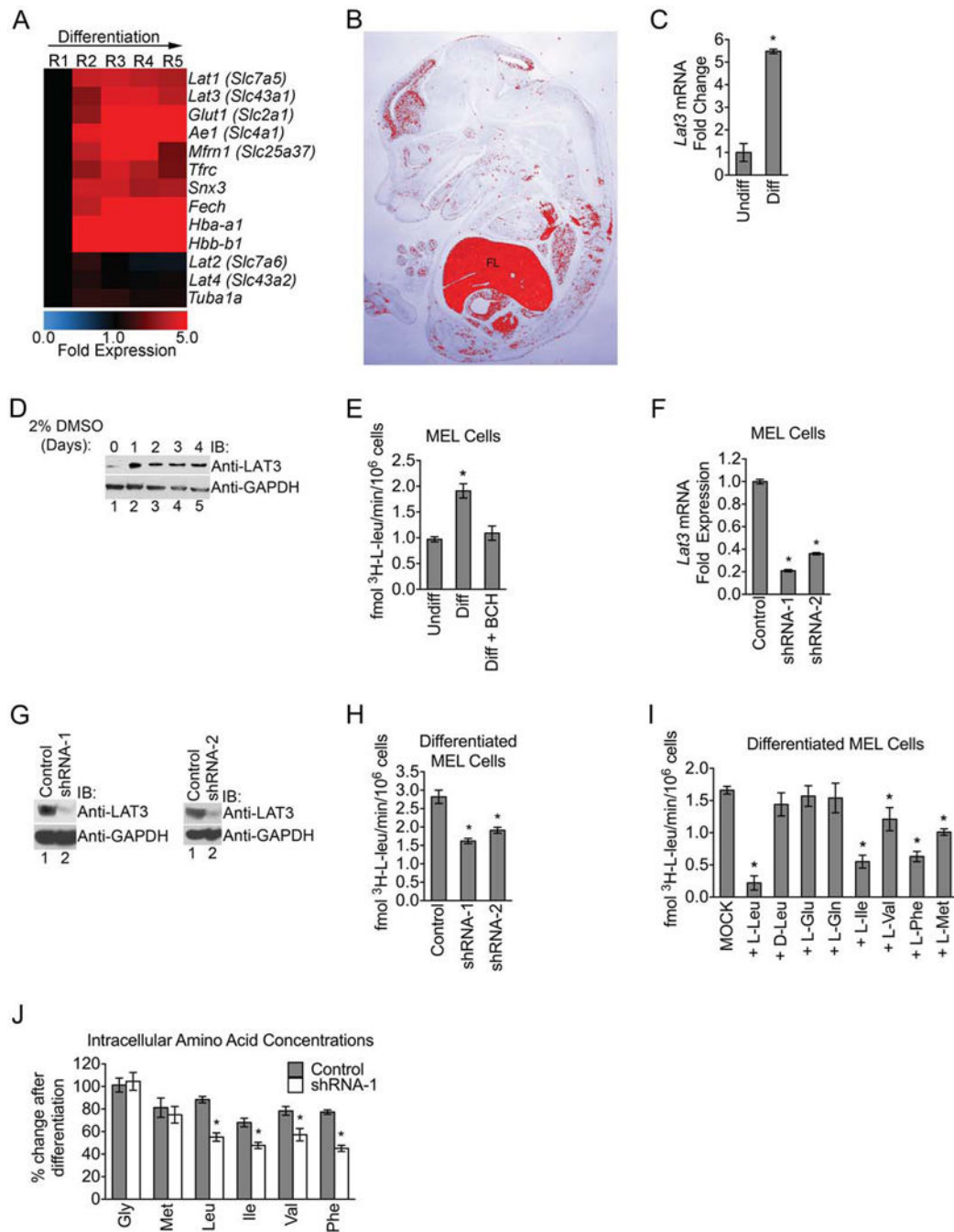
Figure 1. Erythropoiesis involves increased NEAA uptake mediated by increased *Lat3* expression
(**A**) RNAseq gene expression analysis (accession number GSE32110) of fetal liver cells as they mature from R1 to R5 stages, showing induction of LAT3 mRNA with other terminal erythroid transcripts. CD98, the required co-transporter for LAT1 and LAT2, was not detected at any differentiation stage. (**B and C**) *Lat3* mRNA expression was examined in the murine embryo at E14.5 by radiolabelled *in situ* hybridization (pseudo-colored red) (B) and in differentiating MEL cells by qRT-PCR (C), showing enrichment of *Lat3* mRNA in erythropoietic tissues and during erythroid maturation. (**D**) Lysates from undifferentiated
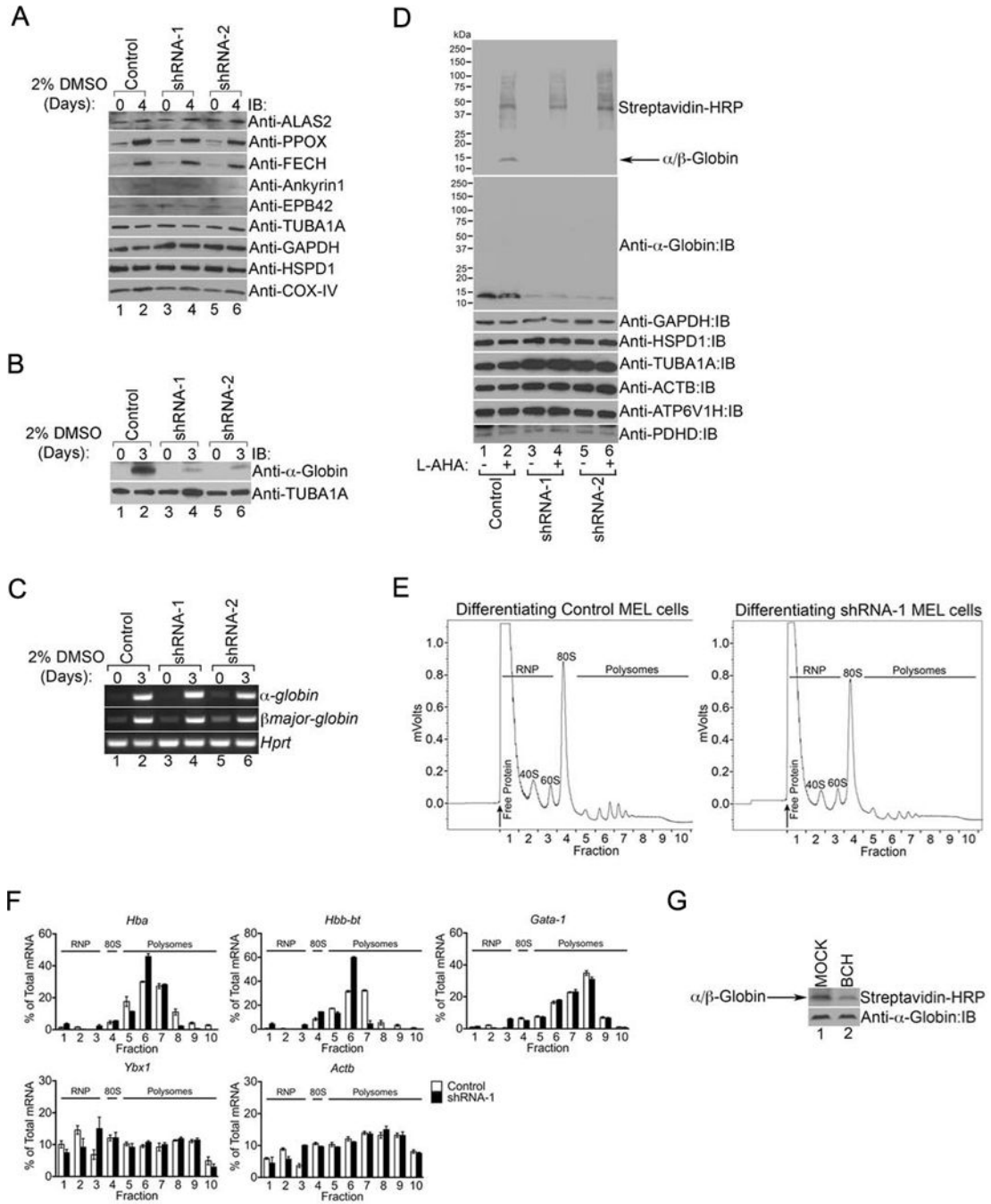
and differentiating MEL cells induced with DMSO at various days were immunoblotted with anti-LAT3 or anti-GAPDH antibodies. **(E to I)** The uptake of [^{3}H]-L-leucine was monitored over 4 minutes in the indicated MEL cell populations (E), in differentiating (Day 3) control or stably *Lat3* shRNA-expressing MEL cells (F to H), or in differentiating (Day 3) MEL cells treated with the indicated non-radioactive amino acids (I). For (I), * denotes significant difference from MOCK treatment. **(J)** GC-MS analysis of maturing MEL cells stably expressing control or *Lat3*-targeting shRNAs. The percentage of each amino acid was normalized to the corresponding undifferentiated samples. *p-value < 0.05. Mean $\pm$ SEM, n = 3 independent experiments for (C), (E), (F), (H), (I), and (J). N= 2 embryos for (B). N= 2 independent experiments for (D) and (G). FL: fetal liver; IB: immunoblot; Undiff: undifferentiated; Diff: differentiated; shRNA: short-hairpin RNA; BCH: 2-aminobicyclo-(2,2,1)-heptane-2-carboxylic acid.
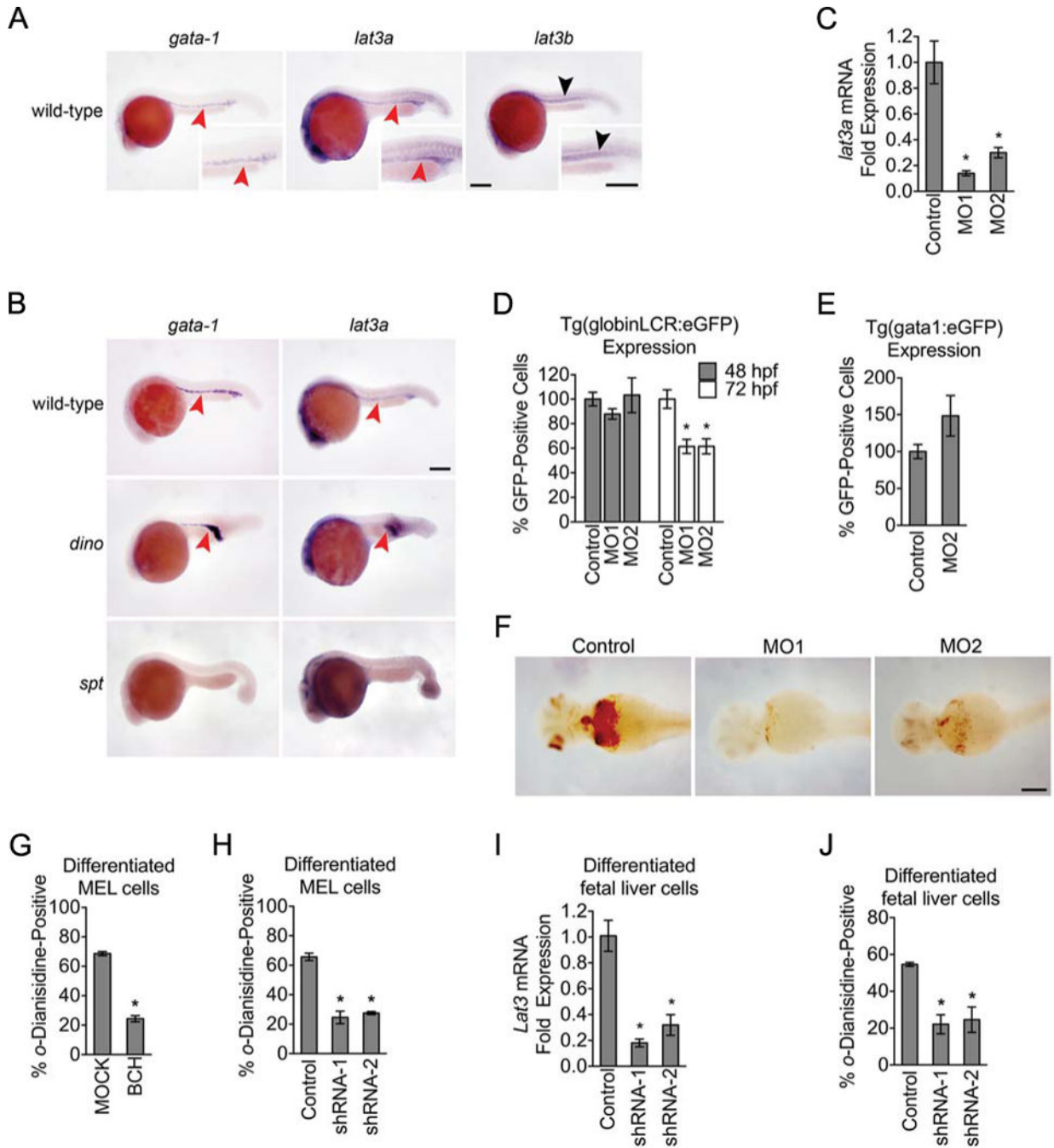
Figure 2. NEAA insufficiency reduces hemoglobinization of erythroid cells
(A and B) *In situ* hybridization using probes specific for *lat3a*, *lat3b*, or *gata-1* was performed on 24 hpf wild-type embryos (A) or mutant fish (B). ICM, red arrowheads; somites are positioned dorsal to the ICM at this developmental stage, black arrowhead. An enlarged view of the posterior ICM is provided in the bottom left corner of each panel (A). Scale bar represents 0.2 μm. **(C to F)** Total RNA was isolated from control or morphant 72 hpf zebrafish embryos and quantitative PCR analysis was performed (C). Control or morphant embryos from Tg(*globin-LCR*:eGFP) (D) or Tg(*gata-1*:eGFP) (E) transgenic lines

were analyzed by flow cytometry. Control or morphant wild-type (F) zebrafish were stained with *o*-dianisidine to examine hemoglobinization at 72 hpf. Scale bar represents 0.2 μm. **(G and H)** *o*-dianisidine staining was performed on MEL cells treated with BCH or control or stably *Lat3* shRNA-expressing MEL cells. **(I to J)** Total RNA was isolated from differentiating fetal liver cells infected with lentiviruses expressing the indicated shRNAs and quantitative PCR was performed (I). These primary fetal liver cells were stained with *o*-dianisidine (J). *p-value < 0.05. Mean ± SEM, n = 3 independent experiments for (C), (D), (E), (G), (H), (I) and (J). Images in (A), (B), and (F) are representative of 2 independent experiments each consisting of at least 40 embryos per condition. shRNA: short-hairpin RNA; MO: morpholino; hpf: hours post-fertilization; BCH: 2-aminobicyclo-(2,2,1)-heptane-2-carboxylic acid.

Figure 3. α/β-globin protein translation is preferentially reduced under limiting NEAA availability

(A and B) Undifferentiated (Day 0) and maturing (Day 3 or 4) control or *Lat3* shRNA expressing MEL cells were lysed and immunoblotted with the indicated antibodies. **(C)** Total RNA was isolated from undifferentiated (Day 0) and differentiating (Day 3) control or *Lat3*-shRNA expressing cells and semi-quantitative RT-PCR analysis for murine *α-globin*, *βmajor-globin*, and *Hprt* was performed. **(D)** Control or *Lat3* shRNA expressing differentiating MEL cells were metabolically labeled with or without L-AHA. Nascent

proteins were visualized by streptavidin-HRP and other proteins were detected by immunoblotting. **(E and F)** Polysome profiling followed by semi-quantitative RT-PCR was performed on differentiating control or *Lat3* shRNA-expressing MEL cells at Day 3 of DMSO differentiation. A representative profile is shown in (E) where the upward arrow represents the start of fraction collection. Densitometry analysis was performed on results from three independent experiments and expressed as a percentage of total RNA (F). The graph shows mean ± SEM. **(G)** Non-radioactive metabolic labeling was performed on differentiating MEL cells (Day 3) treated with BCH. Nascent proteins were visualized using streptavidin-HRP and also immunoblotted with anti-α-globin antibody. n = 2 independent experiments for (A), (B), (D), and (G) and n = 3 for (C). IB: immunoblot; shRNA: short-hairpin RNA; L-AHA: L-azidohomoalanine; HRP: horseradish peroxidase.
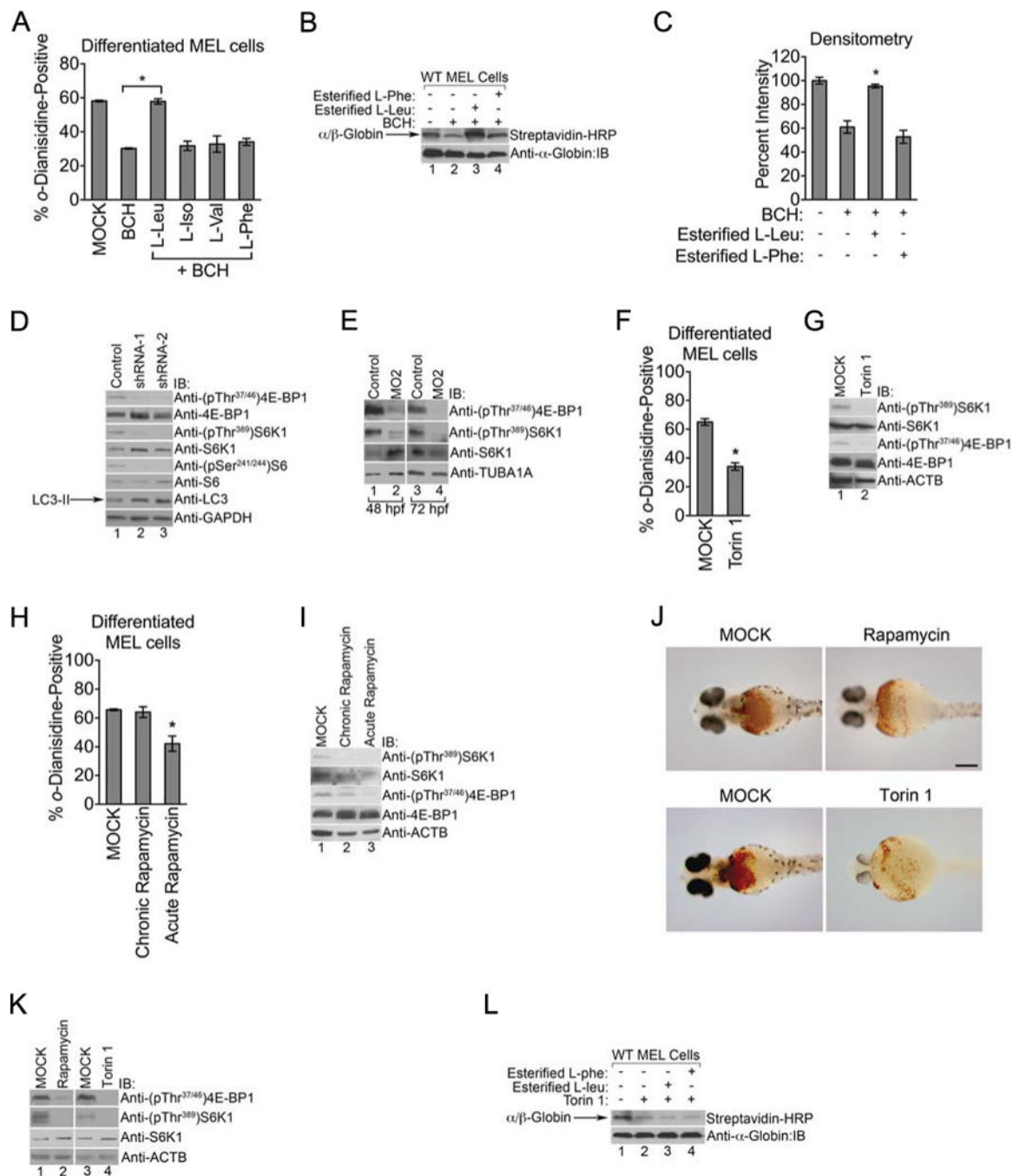
Figure 4. mTORC1 senses sufficient NEAA uptake, particularly L-leucine, in maturing erythroid cells

(**A**) BCH treated MEL cells with or without various amino acid esters starting at Day 0 and were *o*-dianisidine stained for hemoglobinization at Day 4 of differentiation. (**B and C**) Non-radioactive metabolic labeling was performed on Day 3 differentiated MEL cells treated with the indicated combinations of BCH and esterified amino acids (B). Relative protein abundance was quantified by densitometry from three independent experiments and normalized to the total amount of α-globin protein (C). (**D**) Day 3 differentiating control or

Lat3-shRNA expressing cell lysates were immunoblotted with the indicated antibodies. **(E)** Lysates isolated from control or *lat3a*-MO2 injected zebrafish embryos were immunoblotted with the indicated antibodies. **(F to I)** MEL cells were treated with torin 1 (F and G) or rapamycin (H and I) and analyzed by *o*-dianisidine staining (F and H) or western blotting (G and I). **(J and K)** Zebrafish embryos were treated with the indicated compounds and stained with *o*-dianisidine (J) or lysed and analyzed by western blotting (K). Scale bar in (J) represents 0.2 μm. **(L)** Non-radioactive metabolic labeling was performed on Day 3 differentiating MEL cells treated with the indicated combinations of torin 1 and esterified amino acids. *p-value < 0.05. Mean ± SEM, n = 3 independent experiments for (A), (C), (F), and (H). N = 2 independent experiments in (D), (E), (G), (I), (K), and (L). Images in (J) are representative of 2 independent experiments with at least 40 embryos per treatment. IB: immunoblot; shRNA: short-hairpin RNA; L-AHA: L-azidohomoalanine; HRP: horseradish peroxidase.
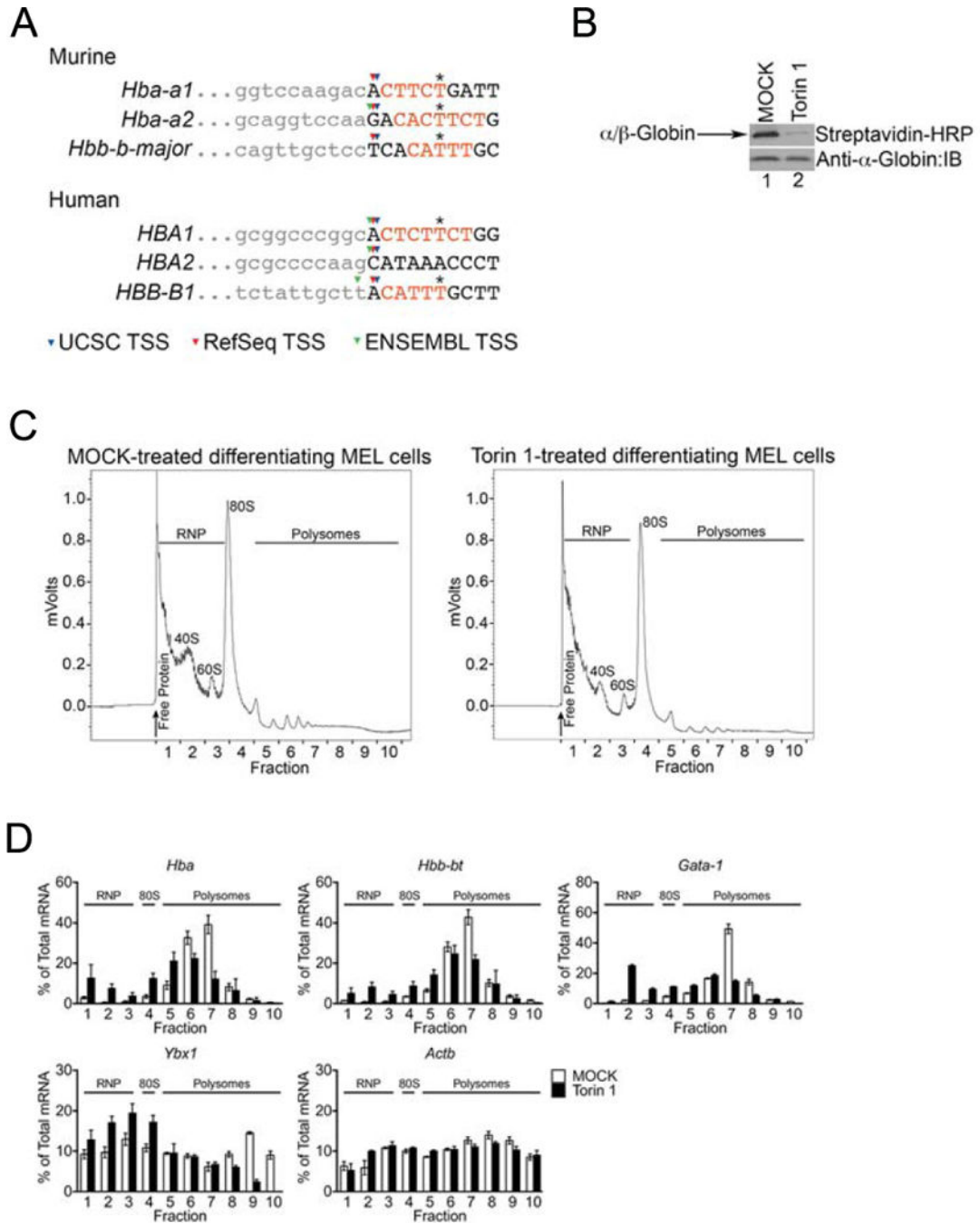
Figure 5. α/β-globin transcripts are direct mTORC1 translational targets
(**A**) The most frequent transcription start site (TSS) of murine and human α/β-globin
mRNAs were analyzed using data from RefSeq, ENSEMBL, and UCSC databases for the
presence of a 5′ terminal oligopyrimidine tract (TOP)-like motif or a pyrimidine rich
translational element (PRTE). (**B**) Non-radioactive metabolic labeling was performed on
differentiating MEL cells (Day 3) treated with torin 1. Nascent proteins were visualized
using streptavidin-HRP and also immunoblotted with anti-α-globin antibody. N = 2
independent experiments. (**C and D**) Polysome profiling and semi-quantitative PCR were

performed on differentiating control or torin 1-treated (2 hours) MEL cells at Day 3 of DMSO differentiation. A representative profile is shown in (C) where the upward arrow denotes the start of fraction collection. Densitometry analysis was performed on results from three independent experiments normalized to total mRNA expression (D). The graph shows mean ± SEM. IB: immunoblot; L-AHA: L-azidohomoalanine; HRP: horseradish peroxidase.
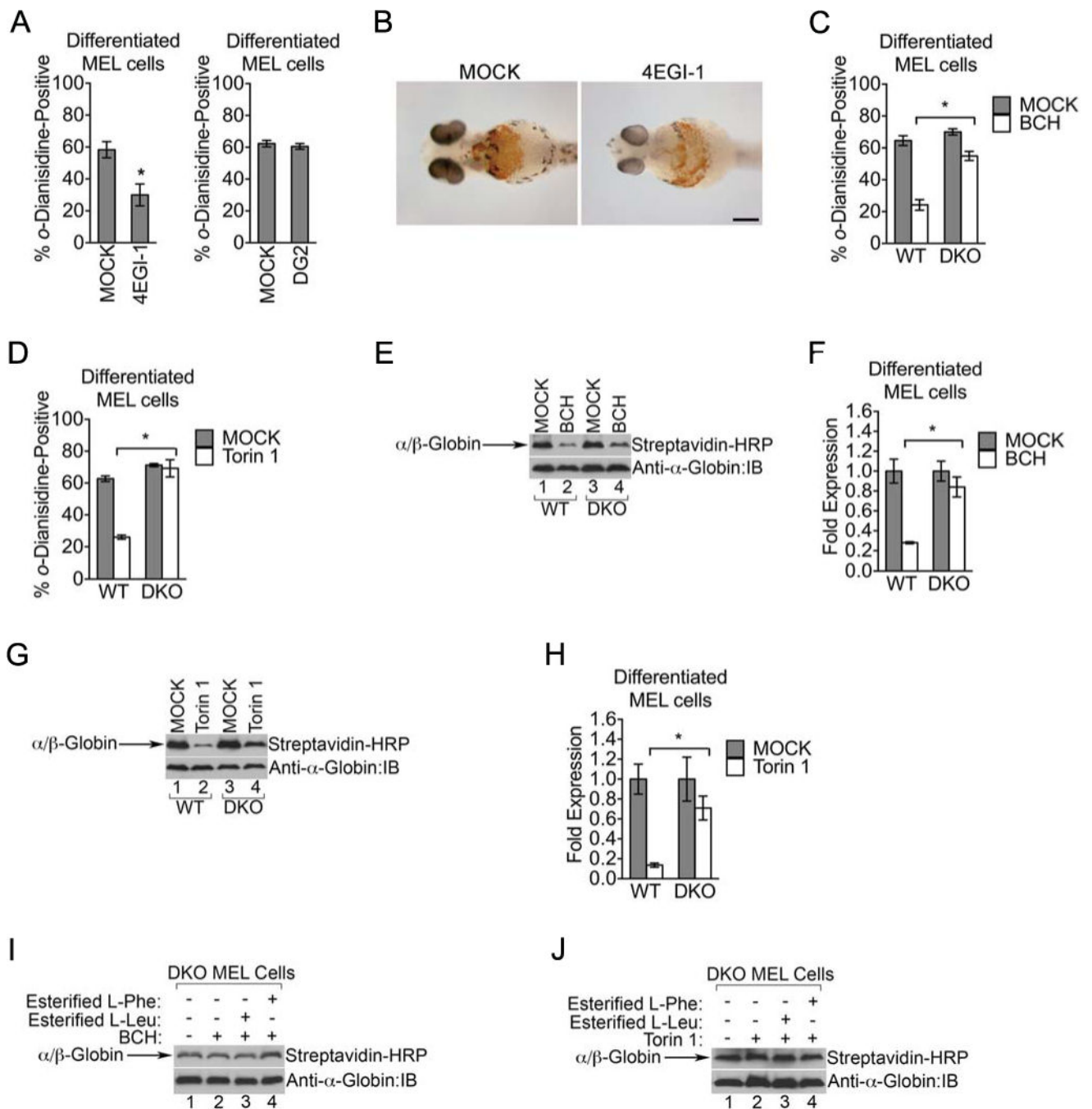
Figure 6. α/β-globin protein translation is regulated by 4E-BP proteins
(**A**) Differentiating MEL cells at Day 4 were stained with o-dianisidine after treatment with 4EGI-1 or DG2. (**B**) Zebrafish embryos at 72 hpf were treated with the 4E-BP mimetic 4EGI-1 and stained for hemoglobinization with *o*-dianisidine. Scale bar represents 0.2 μm. (**C and D**) Wild type or DKO (deficient for both *eif4ebp1* and *eif4ebp2*) MEL cells were differentiated with or without BCH (C) or torin 1 (D) and stained with *o*-dianisidine. (**E to H**) Non-radioactive metabolic labeling experiments were performed with L-AHA on wild type or DKO cells with short-term BCH (E and F) or torin 1 (G and H) treatment. Proteins

were detected by immunoblotting with the indicated antibodies while biotinylated, nascent proteins were detected using a streptavidin-HRP conjugate (E and G). Densitometry analysis was performed on three independent experiments (F and H). Nascent α/β-globin protein synthesis was normalized to α-globin protein expression. **(I and J)** Non-radioactive metabolic labeling was performed on Day 3 differentiated DKO MEL cells treated with the indicated combinations of BCH (I) or torin 1 (J) and esterified amino acids. *p-value < 0.05. Mean ± SEM, n = 3 independent experiments for (A), (C), (D), (F), and (H). Images in (B) are representative of 2 independent experiments with at least 40 embryos per treatment. N= 2 independent experiments for (I) and (J). IB: immunoblot; L-AHA: L-azidohomoalanine; HRP: horseradish peroxidase.
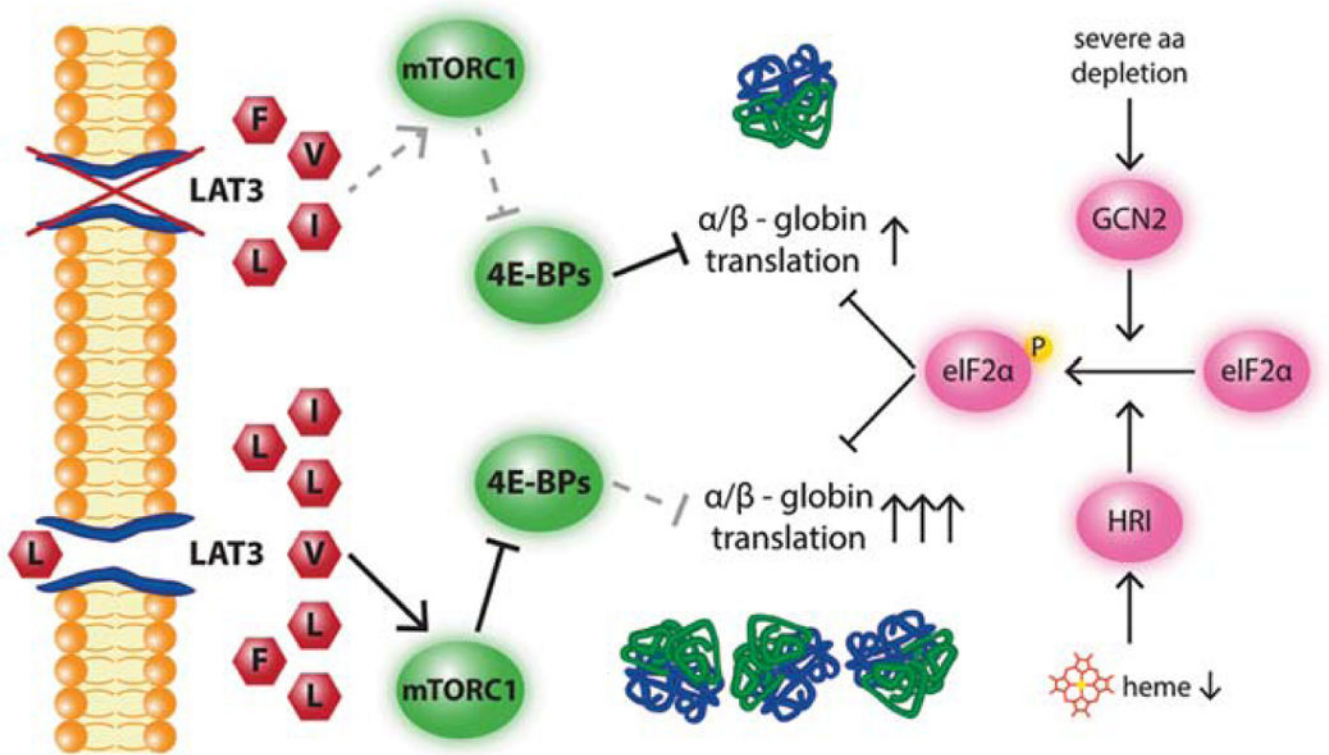
Figure 7. mTORC1 coordinates hemoglobin translation with sufficient NEAA uptake, particularly L-leucine, during erythropoiesis

A schematic depicting our model in which maturing erythroid cells rely on LAT3-mediated NEAA uptake to maintain homeostasis. In the absence of adequate uptake, reduced NEAA content, particularly L-leucine, triggers a reduction in mTORC1/4E-BP signalling and subsequent repression in translation for globin proteins. This mechanism is distinct from the previously identified eIF2α-dependent mechanism that becomes activated with severe amino acid deprivation (GCN2) or heme availability (HRI).